

**TIAM**

Technologia i Automatykacja Montaży

---

**Open Access:** [journals.prz.edu.pl/tiam](https://journals.prz.edu.pl/tiam) • e-ISSN-2450-8217 • Volume 124, Issue 2, 2024

---

Publisher: Łukasiewicz Research Network – Warsaw Institute of Technology • Rzeszow University of Technology • Patronage SIMP • Since 1993



## CONTENTS

---

**3**

**Angelika Arkuszyńska, Jan Godzimirski,  
Marek Rośkiewicz**

**Influence of temperature changes on stresses  
in carbon composite fastening bolts**

*Wpływ zmian temperatury na naprężenia w śrubach  
łączących kompozyty węglowe*

**11**

**Krzysztof Piasta, Jakub Michalski,  
Bartosz Fikus, Przemysław Kupidura**

**Projectile seating depth influence on a small arms  
cartridge performance**

*Wpływ głębokości osadzenia pocisku na  
charakterystyki balistyczne naboju broni strzeleckiej*

**18**

**Dorota Stadnicka, Dario Antonelli**

**Classification Graph of Poka-Yoke Techniques  
for Industrial Applications: Assembly Process  
Case Studies Effectiveness Evaluation**

*Graf Klasyfikacji technik Poka-Yoke do zastosowań  
przemysłowych: Ocena efektywności studiów  
przypadków dla procesu montażu*

**29**

**Tomasz Samborski, Mariusz Siczek, Andrzej  
Zbrowski, Łukasz Łożyński, Stanisław Koziół**

**Compact VOC emission test chamber**

*Kompaktowa komora do badań emisji lotnych  
związków organicznych*

**38**

**Jacek Domińczuk, Małgorzata Gałat**

**Concept of automated car battery assembly line**

*Koncepcja zautomatyzowanej linii montażu baterii  
samochodowych*

**47**

**Marcin Krysiak, Filip Kubik**

**Using Drones and Artificial Intelligence to Assess  
Damage in Aircraft Assembly Joints**

*Użycie dronów oraz sztucznej inteligencji  
w procesie oceny uszkodzeń połączeń montażowych  
samolotu*



Quarterly „Technologia i Automatyzacja Montażu”  
is listed on the list of scored journals of Polish Ministry  
of Education and Science - 40 points.

## INFLUENCE OF TEMPERATURE CHANGES ON STRESSES IN CARBON COMPOSITE FASTENING BOLTS

### WPLYW ZMIAN TEMPERATURY NA NAPRĘŻENIA W ŚRUBACH ŁĄCZĄCYCH KOMPOZYTY WĘGLOWE

Angelika ARKUSZYŃSKA<sup>1,\*</sup> , Jan GODZIMIRSKI<sup>1</sup> , Marek ROŚKOWICZ<sup>1</sup> 

<sup>1</sup> Faculty of Mechatronics, Armaments and Aviation, Military University of Technology, 2 S. Kaliskiego Street, Warsaw, Poland

\* Corresponding author: [angelika.arkuszynska@wat.edu.pl](mailto:angelika.arkuszynska@wat.edu.pl), tel.: +48 261-837-271

#### Abstract

High joint strength of composite structures can be achieved by using mechanical fasteners. The materials used for rivets and bolts have lower coefficients of thermal expansion than composites in the direction perpendicular to the reinforcement fibers. It is suspected, therefore, that temperature changes can cause stress changes in mechanical fasteners. The purpose of this study was to experimentally determine and analytically substantiate the values of stress changes resulting from a change in temperature in the range from -20 to 60°C in M8 steel bolts fastening carbon composite. The value of stress changes was estimated to be around 100 MPa, which can consequently lead to joint unsealing or plastic deformation of the mechanical fastener.

**Keywords:** carbon composites, mechanical fasteners, thermophysical properties, thermal interactions

#### Streszczenie

Wysoka wytrzymałość połączeń struktur kompozytowych może zostać osiągnięta dzięki zastosowaniu łączników mechanicznych. Materiały wykorzystywane do produkcji nitów oraz śrub cechują mniejsze wartości współczynników rozszerzalności cieplnej niż kompozytów w kierunku prostopadłym do włókien zbrojenia. Podejrzewa się więc, że zmiany temperatury mogą powodować zmiany naprężeń w łącznikach mechanicznych. Celem przeprowadzonych badań było eksperymentalne określenie i analityczne uzasadnienie wartości zmian naprężeń wynikających ze zmiany temperatury w zakresie od -20 do 60°C w stalowych śrubach M8 łączących kompozyt węglowy. Wartość zmian naprężeń oszacowano na około 100 MPa, co w konsekwencji może prowadzić do rozszczelnienia połączenia lub plastycznych odkształceń łącznika mechanicznego.

**Słowa kluczowe:** kompozyty węglowe, łączniki mechaniczne, właściwości termofizyczne, oddziaływania termiczne

## 1. Introduction

Carbon Fiber Reinforced Polymers (CFRP) are structural materials that are increasingly replacing metal alloys in the construction of modern aircraft airframes (Kaufmann et al. 2009). This state of affairs is a consequence of the mechanical properties of CFRP composites, especially their high specific strength (strength related to density) and high specific stiffness (Young's modulus related to density). In addition,

these materials are characterized by high fatigue strength and technological susceptibility, which allows the simple manufacture of parts with complex shapes, such as airframe covers with two curvatures (Dipen et al. 2019; Emanoil et al. 2019; Vol'mir et al. 1972; Kamali et al. 2017; Mandalgiri 1999).

Fiber-reinforced composites can have monotropic, orthotropic or quasi-isotropic properties. In each type of these composites there is a direction that is not



reinforced with fibers arranged along that direction. In the case of fabric-reinforced composites (orthotropic and quasi-isotropic), this direction is perpendicular to the fabric surface (Donglin et al. 2023; Ochelski 2004; Hull and Clyne 1996; Ochelski and Gotowicki 2007; Carlsson et al. 2013). In this direction, carbon composites are characterized by a low value of Young's modulus about 6-7 GPa (Ochelski and Gotowicki 2008; Arkuszyńska et al. 2023) and low tensile strength due to the strength of the polymer matrix. Studies show that in this direction the coefficient of linear expansion of the composites at ambient temperature has a value of about  $70 \times 10^{-6}$  1/K. In addition, in this direction the composites exhibit distinct rheological characteristics, including susceptibility to creep (Goertzen and Kessler 2006; Ornaghi et al. 2021).

Composite parts are joined to other composite or metal parts. If the composite parts have low tensile strength and stiffness (thin-walled parts), structural bonding may be a reasonable way of joining (Higgins 2000; Cavalcanti et al. 2021). For higher strength parts, mechanical fasteners such as rivets or bolts should be used. In aeronautical structures, the connections of primary parts (which are decisive for the safety of flying) cannot be only adhesive joints (Gamdani et al. 2022). Studies show the great suitability of adhesive-mechanical hybrid joints for joining composite parts (Nabil et al. 2016). The use of such joints complicates the assembly process due to the need to ensure proper adhesion properties of the surfaces to be joined and proper joint design.

The use of mechanical fasteners requires the drilling of holes in the composite parts to be joined, which creates additional problems, since classical drilling can lead to delamination of the composite and its significant weakening (DeFu et al. 2012; Gaugel et al. 2016; Fernández-Pérez et al. 2017). To avoid these phenomena, special drills or pressure during drilling are used to prevent delamination.

When joining composites using the riveting method, avoid forming the rivet point directly on the composite material, as it may crush. When the rivet is upset, its shank increases in diameter and cancels the clearance between the hole and the rivet. In a riveted lap joint, the composite is loaded mainly on pressure.

Bolted joints used in aircraft construction include special bolts called Hi-Lok. Their distinctive feature is a nut that breaks at a certain torque value, which prevents the allowable pressures from being exceeded during the assembly of the joint (Tomkinson 1991, Yanishevsky et al. 2013). Connections using Hi-Lok fasteners must have a specific length related to the thickness of the package to be joined, which requires having a large assortment of these fasteners. In bolted

connections, the load is carried by frictional forces and, once they are exceeded, by the bolt shanks, which press against the walls of the holes.

Considering that metal fasteners have different thermophysical properties than composite materials, it seems that the preload of bolt fasteners should change as the temperature changes. The purpose of the tests carried out was to see to what extent the stresses in a steel bolt connecting composite elements can change if the temperature varies by  $+40^\circ\text{C}$  and  $-40^\circ\text{C}$  from the assembly temperature,  $20^\circ\text{C}$ . Such temperature changes can occur during aircraft operations.

## 2. Materials and test methods

An orthotropic composite with a thickness of 7.3 mm autoclaved manufactured at the Silesian Science and Technology Center of Aerospace Industry Sp. z o.o. based on GG 204T  $\text{g/m}^2$  IMP 503 ZHT carbon prepreg with a thickness of 7.3 mm, consisting of 25 layers arranged according to the  $[0^\circ]_{25}$  scheme, was tested. The conditions for manufacturing the plate are a pressure of 400 kPa and a curing temperature of  $120^\circ\text{C}$ .

To test the modulus and compressive strength in the  $x_3$  axis direction (the axis perpendicular to the arrangement of the layers of composite material, 7 cubes measuring  $27 \times 27 \times 7.3$  mm with 10.1 mm diameter holes were bonded together (Figure 1).



**Fig. 1.** A cube cut from the tested composite

A specimen with a height of 52 mm and a cross-sectional area of  $633 \text{ mm}^2$  was obtained, which was loaded with a force of up to 250,000 N, and the dependence of the displacement of the crosshead of the machine (Instron 8802) as a function of force was recorded (Figure 2). In addition, the stiffness characteristics of the testing machine were determined by compressing its platens without the specimen (Figure 3).

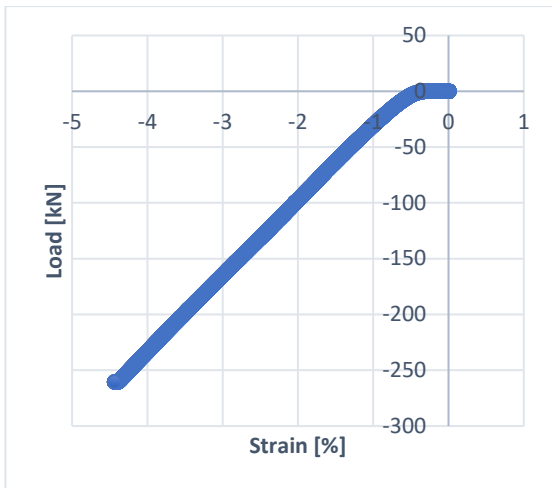


Fig. 2. Compression curve of the composite specimen

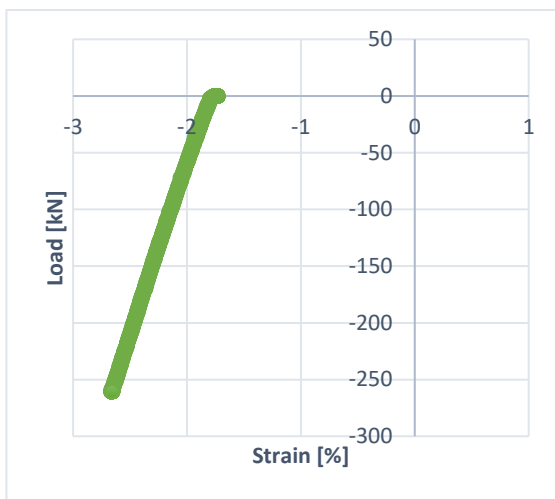


Fig. 3. Stiffness characteristics of the Instron 8802 testing machine

Based on the two compression curves obtained, the value of Young's modulus of the tested orthotropic composite in the  $x_3$  direction, that is, in the direction of compression of the material by the bolt, was calculated. The modulus was estimated at 6240 MPa.

A CL20M8 force sensor with a measuring range of 10 kN (ZEPWN J. Czerwinski & Associates) was used to test the tensile force of the bolt. First, it was examined to what extent a temperature change of  $\pm 40^\circ\text{C}$  affects the force measurement. The M8 bolt itself was tightened in the sensor to such a torque that a gauge reading of 6000 N was obtained (stresses in the bolt 183 MPa).

The effect of elevated temperature was studied by holding the force sensor specimen in a laboratory dryer by heating its chamber to  $60^\circ\text{C}$ , and the effect of reduced temperature – by holding the specimen in a freezer for one hour. The measurements showed, that there was an increase of 120 N in the increased temperature, and a decrease of 230 N in the reduced

temperature. Thus, the change in force did not exceed 4%. These values were considered by changing the force values recorded when testing the composite. Hence, for the purposes of this study, the notion of registered force and actual force was defined, the value of which was calculated by correcting the measured value by the deviation determined experimentally and generated by the sensor itself at variable temperature.

The effect of elevated temperature on the screw-sensor system was studied by holding the force-sensor sample in a laboratory dryer heated to  $60^\circ\text{C}$ , and the effect of reduced temperature was studied by holding the sample in a freezer for one hour. The measurements showed that there was an increase in force of 120 N at the increased temperature, and a decrease of 230 N at the reduced temperature. Thus, the change in force did not exceed 4%. These values were taken into account by subtracting them from the force values recorded when testing the composite, and the real forces were obtained.

To study the change of stress in the bolt loading the composite material, 4 cubes of  $27 \times 27 \times 7.3$  mm (Figure 4) and 1 cube of the same dimensions (Figure 5) were used, in which 8.1 mm diameter holes were drilled centrally. These cubes were applied to an M8 bolt and, in addition, a force measurement sensor was used. The nut was tightened to such a torque that a clamping force of 6000 N was obtained.



Fig. 4. Four composite cubes and a load cell bolted together with an M8 screw



Fig. 5. One composite cube and force sensor bolted together with an M8 screw

The changes in clamping force with time and at elevated and depressed temperatures were then checked.

### 3. Test results

First, the change in bolt force at ambient temperature of a specimen with a composite package thickness of 29.5 mm was checked (Table 1).

An approximate 9% decrease in strength due to composite creep was found.

**Table 1.** Variation of compression bolt tension of 29.5 mm thick composite package as a function of time at ambient temperature

Time [h]	Recorded force [N]
0	6000
0,5	5770
18	5470

The results of further testing of the specimen at different temperatures are given in Table 2.

**Table 2.** Variation of compression bolt tension of 29.5 mm thick composite package as a function of time and temperature

Temperature [°C]	Time [h]	Recorded force [N]	Real force [N]
60	1	6630	6510
20	0,5	4800	4800
60	0,5	6470	6350
	1	6220	6220
20	1	4150	4150
60	1	6080	5960
20	50	4160	4160
60	1	6060	5940
-20	1	2310	2540
60	1	5970	5850
-20	1	2240	2470
60	1	5900	5780
20	18	3960	3960
60	1	5890	5770

Subsequently, similar tests of the change in screw clamping force at ambient temperature (20°C) and at variable temperature (20°C, 60°C, -20°C) were carried out for a 7.3 mm thick composite. The results are shown in Tables 3 and 4, respectively.

In tests at ambient temperature (20°C), there was about a 3.7% decrease in strength due to composite creep.

**Table 3.** Variation of compression bolt tension of 7.3 mm thick composite as a function of time at ambient temperature

Time [h]	Recorded force [N]
0	6000
0,5	5930
18	5780

**Table 4.** Variation of compression screw tension of 7.3 mm thick composite as a function of time and temperature

Temperature [°C]	Time [h]	Recorded force [N]	Real force [N]
60	0,5	6480	6360
	1	6390	6270
20	0,5	5300	5300
60	1	6280	6160
20	1	5190	5190
60	1	6200	6080
20	1	5120	5120
-20	1	3970	4200
60	1	6150	6030
20	18	5190	5190
-20	1	4010	4240
60	1	6140	6020
-20	1	3970	4100

**Table 4 (cont.).** Variation of compression screw tension of 7.3 mm thick composite as a function of time and temperature

Temperature [°C]	Time [h]	Recorded force [N]	Real force [N]
60	1	6040	5920
20	0.5	5080	5080
20	18	5040	5040
20	70	5080	5080
20	24	5110	5110
20	24	5020	5020

#### 4. Analysis of test results

The tests showed a significant effect of temperature change on the value of the force with which the bolt compressed the tested composite or its package. The tests also show that with the applied load (force of 6000 N, washer pressure on the composite of

41.6 MPa) there was creep of the composite already at ambient temperature, resulting in a decrease in force from 6000 N to 5470 N in 18 hours for a composite package of 29.5 mm thickness and from 6000 N to 5780 for a composite of 7.3 mm thickness (Figure 6).

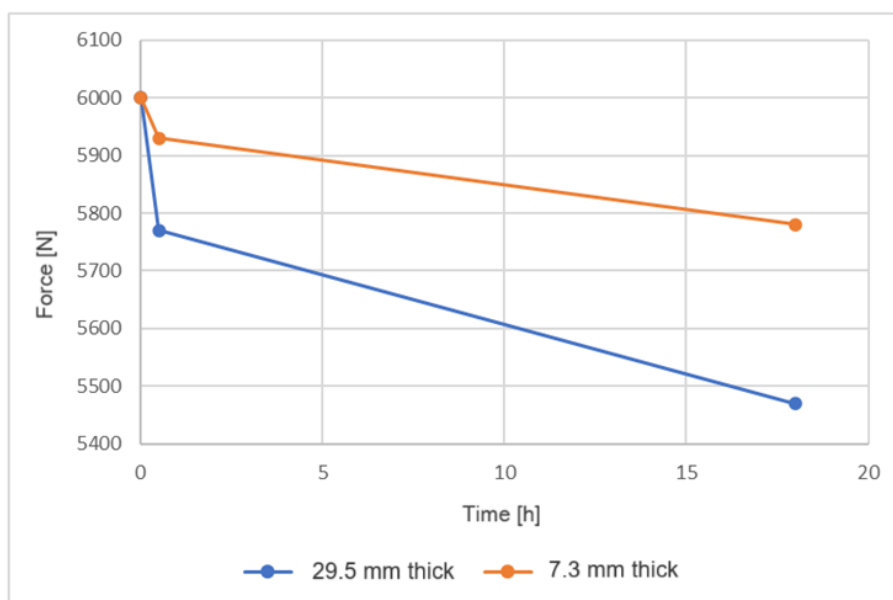


**Fig. 6.** Change in time of the forces with which the screw compressed the composite of different thicknesses at ambient temperature

Heating the tested composite package joint by 40°C increased the force from 5470 N to 6510 N. Taking into account the height of the composite package (29.5 mm) and the length of the bolt shaft (46 mm resulting from the height of the composite package and the height of the force sensor), the difference in thermal deformation of the composite and the bolt was calculated.

$$\Delta l = l \times \alpha \times \Delta T \tag{1}$$

where:  $l$  - height of the composite package/ length of the bolt shaft,  $\alpha$  - thermal expansion coefficient,  $\Delta T$  - temperature change.

$$\Delta l_c = 29.5 \times 70 \times 10^{-6} \times 40 = 0.0826 \text{ mm} \tag{2}$$

$$\Delta l_b = 46 \times 11 \times 10^{-6} \times 40 = 0.0203 \text{ mm} \tag{3}$$

$$\Delta l_{c-b} = 0.0826 - 0.0203 = 0.0623 \text{ mm} \tag{4}$$

The calculated strain is the sum of the deformations of the bolt and the composite. These deformations are inversely proportional to the tensile stiffness of the joint components. The actual strain of the composite ( $\Delta l_{cr}$ ) can be calculated from the relationship:

$$\frac{\Delta l_{cr}}{\Delta l_{c-b} - \Delta l_{cr}} = \frac{A_b \times E_b}{A_w \times E_c} \tag{5}$$

where:  $E_b$  - Young's modulus of the bolt (steel),  $E_c$  - Young's modulus of the composite,  $A_b$  - cross-sectional area of the bolt M8,  $A_w$  - area of the bolt washer M8.

$$\frac{\Delta l_{cr}}{0.0623 - \Delta l_{cr}} = \frac{32.8 \times 200}{144.2 \times 6.24} \quad (6)$$

$$\Delta l_{krz} = 0.0548 \text{ mm} \quad (7)$$

The real deformation of the bolt can be calculated from the relationship:

$$\Delta l_{br} = \Delta l_{c-b} - \Delta l_{cr} = 0.0075 \text{ mm} \quad (8)$$

The stress increment in the bolt due to its elongation can be calculated from Hooke's law:

$$\Delta \sigma = \frac{\Delta l_{br}}{l_b} \times E = \frac{0.0075}{46} \times 200000 = 32.6 \text{ MPa} \quad (9)$$

The force increment is the product of the stress increment and the bolt's cross-sectional area:

$$\Delta F = \Delta \sigma \times A_b = 32.6 \times 32.8 = 1070 \text{ N} \quad (10)$$

The calculated value of the force increment is close to the value derived from the experiment:

$$6510 - 5470 = 1040 \text{ N} \quad (11)$$

The study also showed that during the loading of the composite package with a thickness of 29.5 mm at different temperature there was a continuous slow decrease in the recorded forces which was caused by creep of the composite material. A decrease in force at ambient temperature was found from 5470 N to 3960 N, or about 28%. Such a large deformation of the composite associated with its creep was due, among other things, to the large thickness of the tested package.

The difference in the compressive force of the 29.5-mm-thick composite package at 60°C and -20°C was 3310 N, resulting in a change in the bolt stress of about 100 MPa from 176.2 to 75.3 MPa.

When the 7.3-mm-thick composite was loaded, there was also a decrease in recorded forces at ambient temperature, but in a smaller range from a force of 5780 N to 5190 N, and thus by about 10%. This is as expected, since the permanent deformation resulting from creep of the thinner composite has a lower value.

The difference in the compressive force of the 7.3-mm-thick composite package at 60°C and -20°C was 1,790 N, resulting in a change in the stress in the bolt of about 54.5 MPa from 183.8 to 129.3 MPa.

The differences in the changes in compression forces of the composites associated with changes in temperature from from +40 to -20°C determined for composites of different thicknesses are because for the two cases considered, the ratio of the active length of the bolt (thickness of the composite plus thickness of the sensor) to the thickness of the composite was different. For a composite of 7.3 mm thickness it was 3.26, and for a composite package of 29.5 mm

thickness it was 1.56. In real joints, if we ignore the thickness of the washer, this ratio is 1. It follows that temperature changes in the considered range will cause more than 28% changes in the compressive forces of real joints of composite materials. Making simplifying assumptions that in the considered range of temperature changes the coefficient of linear expansion of the composite and the value of its Young's modulus do not change, and that the composite deforms uniformly under the washer, it is possible to estimate the range of changes in the forces acting on the M8 bolt under the influence of temperature changes.

$$\Delta l_c = l \times 70 \times 10^{-6} \times 80 = 0.0056 \times l \text{ mm} \quad (12)$$

$$\Delta l_b = l \times 11 \times 10^{-6} \times 80 = 0.00088 \times l \text{ mm} \quad (13)$$

$$\Delta l_{c-b} = (0.0056 - 0.00088)l = 0.00472 \times l \text{ mm} \quad (14)$$

$$\frac{\Delta l_{cr}}{\Delta l_{c-b} - \Delta l_{cr}} = \frac{A_b \times E_b}{A_w \times E_c} \quad (15)$$

$$\frac{\Delta l_{krz}}{0.00472 \times l - \Delta l_{krz}} = \frac{32.8 \times 200}{144.2 \times 6.24} = 7.29 \quad (16)$$

$$\Delta l_{cr} = 0.00415l \text{ mm} \quad (17)$$

$$\Delta l_{br} = \Delta l_{c-b} - \Delta l_{cr} = 0.00057l \text{ mm} \quad (18)$$

$$\Delta \sigma = \frac{\Delta l_{br}}{l_b} \times E = \frac{0.00075l}{l} \times 200000 = 114 \text{ MPa} \quad (19)$$

$$\Delta F = \Delta \sigma \times A_b = 114 \times 32.8 = 3740 \text{ N} \quad (20)$$

In an M8 bolt, the range of force change due to temperature change by 80°C will be at 3740 N. The range of stress change in steel bolts (about 114 MPa) should depend little on the diameter of the bolt, and only to some extent on the dimensions of the washers.

To check the validity of the analysis, numerical calculations of the effect of temperature change on the value of stresses in the bolt connecting the composite material were carried out. The calculations were carried out in ANSYS 19.2. A numerical model of a 7.3-mm-thick composite specimen with a hole  $d = 8.1$  mm was built, in which an M8 steel bolt was placed. In the built model, the bolt head and nut were modeled as cylinders with washer diameter ( $d = 16$  mm) and thickness of 4 mm. The specimen model with a grid of elements is shown in Figure 7.

The mechanical and physical properties of the steel were taken from the ANSYS system library. The properties of the composite were declared based on tests performed and data from the system's library of composite materials (Table 5).



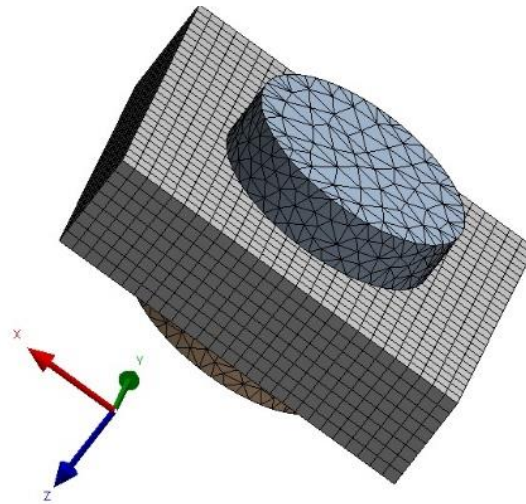


Fig. 7. Grid of elements of the analyzed specimen

Table 5. Material constants of the composite adopted for numerical calculations

$E_x$ [GPa]	$E_y$ [GPa]	$E_z$ [GPa]	$\nu_{xy}$ [-]	$\nu_{yz}$ [-]	$\nu_{xz}$ [-]	$G_{xy}$ [GPa]	$G_{yz}$ [GPa]	$G_{xz}$ [GPa]	$\alpha_z$ [1/K]
30,00	30,00	6,24	0,04	0,30	0,30	18,00	2,70	2,70	$5 \times 10^{-5}$

There was a gap between the bolt shaft and the hole. A ‘no separation’ contact was declared between the surfaces of the cylinders mapping the head and nut with washers and the surfaces of the composite cube. The outer surface of one cylinder was deprived of the possibility of movement. All elements of the specimen were loaded with a temperature change by 80°C. The average normal stress in the bolt shaft after the temperature change was about 100 MPa (Figure 8), which was about 14% lower than that resulting from analytical calculations (114 MPa for the same temperature change by 80°C).

B: Copy of Static Structural  
 Normal Stress  
 Type: Normal Stress(Z Axis)  
 Unit: MPa  
 Global Coordinate System  
 Time: 1  
 05.12.2023 11:32

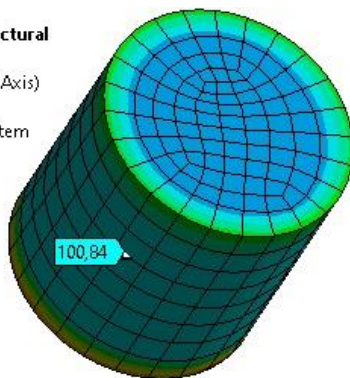


Fig. 8. Normal stresses in the bolt shank of the specimen loaded with a temperature increment of 40°C

The results of the numerical calculations should be considered more reliable due to the simplifying assumptions made in the analytical calculations,

including the assumption that the composite deforms uniformly under the washer.

### 5. Conclusions

Mechanical fasteners (bolts and rivets) used to join composite parts are most often positioned perpendicular to the fiber laying plane. In this direction, composite materials are characterized by a low value of Young's modulus - a few GPa (Ochelski and Gotowicki 2008) and a relatively high value of the coefficient of linear expansion.

In stressed bolts connecting composite parts, there is a decrease in stress over time, resulting in a decrease in the value of the clamping force of the parts being joined. This is due to the rheological properties of the polymer matrix of the composites, which result in composite creep. With the passage of time, the intensity of creep, like that of other materials, such as steel alloys (Bolanowski 2013) - decreases. Increased temperature accelerates the creep process.

Approximately seven times the value of the coefficient of linear expansion of composites in the plane perpendicular to the stacked fibers ( $70 \times 10^{-6}$  1/K) than the coefficient of linear expansion of steel ( $1.1 \times 10^{-6}$  1/K) results in stress changes in the bolts as the temperature changes. An increase in temperature relative to the joint assembly temperature results in an increase in stress, while a decrease in temperature results in a decrease in stress.

Experimental studies and analyses show that in the case of a carbon-epoxy composite joined by steel bolts,

changes in temperature in the range from +60 to -20°C cause stress changes in the range of 100 MPa. Such large stress changes can significantly affect the strength of the connections, cause them to unseal or load the bolt with a force that causes the material to exceed its yield strength.

To reduce the range of stress changes in bolts connecting composite materials resulting from changes in the temperature of the joint, bolts should be made from materials whose value of the coefficient of thermal expansion is more similar to the value of this feature of the composite, such as from aluminum alloys ( $25 \times 10^{-6}$  1/K).

### Acknowledgments

**Funding:** This work was financed by Military University of Technology under research project UGB 735/2024.

### References

- Arkuszyńska A., Godzimirski J., Rośkiewicz M. (2023). Analysis of the properties of orthotropic composites in terms of their use in airframe repairs. *Technologia i Automatykacja Montażu* 121, 3-12.
- Bolanowski K. (2013). Właściwości wytrzymałościowe oraz zmiany morfologii mikrostruktury stali mikrostopowej w warunkach pełzania. *Monografie, Studia, Rozprawy (Wydawnictwo Politechniki Świętokrzyskiej)* 39.
- Carlsson L.A., Adams D. F., Pipes B. R. (2013). Basic Experimental Characterization of Polymer Matrix Composite Materials. *Polymer Review* 53, 277-302.
- Cavalcanti W. L., Brune K., Noeske M., Tserpes K., Ostachowicz W. M., Schlag M. (2021). *Adhesive Bonding of Aircraft Composite Structures. Non-destructive Testing and Quality Assurance Concepts*. Cham: Springer.
- DeFu L., YongJun T., Cong W.L. (2012). A review of mechanical drilling for composite laminates. *Composite Structures* 94, 1265-1279.
- Dipen R. K., Durgesh P. D., Ravinder K., Catalin P. I. (2019). Recent progress of reinforcement materials: a comprehensive overview of composite materials. *Journal of Materials Research and Technology* 8(6), 6354-6374.
- Donglin G., Zuguo B., Weijian H., Xianpeng W., Shiyao H., Li H., Qiuren Ch., Hailong Z., Yahong X. (2023). Effect of Strain Rate on Tensile Properties of Carbon Fiber-Reinforced Epoxy Laminates with Different Stacking Sequences and Ply Orientations. *Polymers* 15, 2711.
- Emanoil L., Dipen R. K., Durgesh P. D., Pradeep M. L. (2019). Fiber-Reinforced Polymer Composites: Manufacturing, Properties, and Applications". *Polymers* 11(10), 1667
- Fernández-Pérez J., Cantero J. L., Díaz-Álvarez J., Miguélez M. H. (2017). Influence of cutting parameters on tool wear and hole quality in composite aerospace components drilling. *Composite Structures* 178, 157-161.
- Gamdani F., Boukhili R., Vadean A. (2022). Fatigue behavior of hybrid multi-bolted-bonded single-lap joints in woven composite plates. *International Journal of Fatigue* 158, 106738.
- Gaugel S., Sripathy P., Haeger A., Meinhard D., Bernthaler T., Lissek F., Kaufeld M., Knoblauch V., Schneider G. (2016). A comparative study on tool wear and laminate damage in drilling of carbon-fiber reinforced polymers (CFRP). *Composite Structures* 155, 173-183.
- Goertzen W. K., Kessler M. R. (2006). Creep behavior of carbon fiber/epoxy matrix composites. *Materials Science and Engineering A* 421, 217-225.
- Higgins A. (2000). Adhesive bonding of aircraft structures. *International Journal of Adhesion & Adhesives* 20, 367-376.
- Hull D., Clyne T. W. (1996). *An Introduction to Composite Materials*. Cambridge: Cambridge University Press.
- Kamali G., Ashokkumar N., Sugash K., Magesh V. (2017). Advanced Composite Materials of the Future in Aerospace Engineering. *International Journal for Research in Applied Science & Engineering Technology* 5, 610-614.
- Kaufmann M., Zenkert D., Wennhage P. (2009). Integrated cost/weight optimization of aircraft structures. *Structural and Multidisciplinary Optimization* 41(2), 325-334.
- Mandalgiri P. D. (1999). Composite Materials for Aerospace Applications. *Bulletin of Materials Science* 22(3), 657-664.
- Nabil V., Reyes L. A., Hernández-Muñoz G.M., Zambrano-Robledo P. (2016). Parametric Effects in Hybrid Lap Joints of Composite Materials Used in Aircraft Structures. *W Proceedings of the Symposium of Aeronautical and Aerospace Processes, Materials and Industrial Applications*. Springer.
- Ochelski S. (2004). *Metody doświadczalne mechaniki kompozytów konstrukcyjnych*. Warszawa: Wydawnictwa Naukowo-Techniczne.
- Ochelski S., Gotowicki P. (2007). Doświadczalna ocena zdolności pochłaniania energii kompozytów węglowo-epoksydowych i szklano-epoksydowych. *Biuletyn WAT LVI*(1), 143-158.
- Ochelski S., Gotowicki P. (2008). Experimental Support for Numerical Simulations of Energy Absorbing Structures. *Journal of KONES Powertrain and Transport* 15(1), 183-217.
- Ornaghi H. L., Almeida J. H. S., Monticeli F. M., Neves R. M., Cioffi M. O. H. (2021). Time-temperature behavior of carbon/epoxy laminates under creep loading. *Mech Time-Depend Mater* 25, 601-615.
- Tomkinson G. (1991). *Hi-Lok and Hi-Lok/Hi-Tigue Fasteners Installations Instructions*. Hi-Shear Corporation.
- Vol'mir A. S., Pavlenko V. F., Ponomarev A. T. (1972). Use of composite materials in airframes. *Polymer Mechanics* 8, 89-95.
- Yanishevsky M., Gang L., Shi G., Backman D. (2013). Fractographic examination of coupons representing aircraft structural joints with and without hole cold expansion. *Engineering Failure Analysis* 30, 74-90.

## PROJECTILE SEATING DEPTH INFLUENCE ON A SMALL ARMS CARTRIDGE PERFORMANCE

### WPLYW GŁĘBOKOŚCI OSADZENIA POCISKU NA CHARAKTERYSTYKI BALISTYCZNE NABOJU BRONI STRZELECKIEJ

Krzysztof PIASTA<sup>1\*</sup>, Jakub MICHALSKI<sup>1</sup>, Bartosz FIKUS<sup>1</sup>,  
Przemysław KUPIDURA<sup>1</sup>

<sup>1</sup> Military University of Technology, Faculty of Mechatronics, Armament and Aviation, 2 Sylwestra Kaliskiego Str., 00-908 Warsaw, Poland

\* Corresponding author: e-mail: [krzysztof.piesta@wat.edu.pl](mailto:krzysztof.piesta@wat.edu.pl)

#### Abstract

In the world of small-arms ammunition, precision reigns supreme. The most significant feature of ammunition for shooters is undoubtedly the repeatability from one shot to the next. This study explores the detailed assembly process of small arms cartridges, leveraging modern machinery and innovative designs employed by cartridge manufacturers. It emphasizes how these tools ensure the fundamental repeatability and precision necessary for the quality of each batch of rounds. Establishing standards for the highest possible quality requires assessing the impact of imprecise cartridge assembly on ballistic performance.

Utilizing a free-flight ballistic tunnel, a high-speed camera, light- and target-screen systems, the authors analyzed the effects of varying projectile seating depths thus affecting cartridge overall lengths (COAL) and cartridge base to ogive distance (CBTO) on the initial velocity and shot dispersion at 50 meters. The study was conducted for two types of projectiles, differing in their ogive profiles: secant and tangent ogive. The performance differences between these profiles provided valuable insights for future projectile designs, highlighting that low-drag projectiles are slightly more sensitive to the seating depth than tangent profile bullets, and the importance of it should be considered in mass, military production as well. It is a valuable resource for analyzing the trade-off between producing bullets with a low drag coefficient and ensuring high precision. The research enhances the understanding of internal and external ballistics but most importantly draws attention to the importance of the standards of assembly processes to ensure optimal performance and safety in the field.

**Keywords:** mechanical engineering, ballistics, ammunition design, cartridge assembly, projectile

#### Streszczenie

Zapewnienie powtarzalności między kolejnymi strzałami jest niewątpliwie najistotniejszą cechą naboju dla każdego strzelca. Autorzy poddali analizie proces montażu naboju do broni strzeleckiej, wykorzystując nowoczesne maszyny i innowacyjne rozwiązania konstrukcyjne stosowane przez światowych producentów amunicji. Biorąc pod uwagę jakość wykonanej amunicji, te narzędzia są wykorzystywane do zapewnienia jak największej dokładności i powtarzalności, które są fundamentalne w kwestii kontroli jakości partii naboju. W celu wypracowania odpowiedniego standardu zapewniającego wymaganą jakość amunicji, istotne jest oszacowanie wpływu nieprecyzyjnego montażu naboju na ich charakterystyki balistyczne.

Przeprowadzając badania w tunelu balistycznym z wykorzystaniem kamery szybkiej oraz bramek prędkościowych i współrzędnościowych, przeanalizowano wpływ zmiennej głębokości osadzenia pocisku, a więc również całkowitej długości naboju (COAL) oraz odległości od dna łuski do części ostrołukowej (CBTO) na prędkość wylotową rozrzut pocisków na odległości 50 metrów. Analizy przeprowadzono dla różnych typów pocisków, różniących się kształtem części ostrołukowej. Wpływ różnic w ich konstrukcji na charakterystyki balistyczne jest istotny pod względem przyszłościowych naboju, ponieważ pociski o mniejszym współczynniku oporu czołowego – większym promieniu profilu części ostrołukowej, są wrażliwsze na głębokość osadzenia, niż pociski o profilu ostrołuku styczonym do części cylindrycznej, które charakteryzują się większym współczynnikiem oporu czołowego. Analizowane różnice okazują się istotne również w masowej produkcji

amunicji wojskowej. Wyniki stanowią cenne źródło informacji w poszukiwaniu kompromisu między produkcją pocisków o niskim współczynniku oporu aerodynamicznego, a zapewnieniem wysokiej precyzji. Praca pogłębia zrozumienie balistyki wewnętrznej i zewnętrznej, ale przede wszystkim zwraca uwagę na znaczenie jakości procesu montażu amunicji w kwestii zapewnienia optymalnej skuteczności zastosowania i bezpieczeństwa na polu walki.

**Słowa kluczowe:** inżynieria mechaniczna, balistyka, amunicja, montaż nabojów pośrednich, pocisk

## 1. Introduction

In the domain of small-arms ammunition manufacturing and elements production, precision plays a key role. Consideration of the geometric restrictions and accurate dimensions was a subject of various analyses and is thoroughly understood in the long-range shooting community. However, the aspect of precision with which a bullet is seated into its cartridge case is still of utmost importance, specifically in case of military use, where the ammunition is produced and assembled on a mass scale. Especially in the case of long-range precision shooting, the small differences in the performance of cartridges in an ammunition batch play a vital role.

The process of bullet seating is influenced by several factors, including the design of the cartridge elements itself. Small-arms cartridges are manufactured in a variety of designs, from the widely used centerfire and rimfire cartridges to specialized configurations like ammunition with semi-jacketed, boattailed projectiles and hybrid steel-brass cases. Each design presents its own set of challenges in achieving consistent dimensions due to differences in the mechanical interaction between the bullet, case, and seating machinery (Frost, 1990).

The main parameters used for specifying how deep the bullet should be placed inside the cartridge case, are the cartridge's overall length (COAL) and cartridge base to ogive distance (CBTO). COAL is the distance between the base of the cartridge case and the bullet's tip – méplat. On the other hand, CBTO is the distance between the cartridge case base to the point where the bullet's ogive starts (Fig. 1). CBTO is specifically a critical measurement directly related to the precision of the cartridge. It can be used to characterize the distance that a bullet moves when fired, before its surface engages the barrel rifling.

Considering the projectile's geometry, the most difficult part to manufacture repetitively is its méplat. Moreover, it is problematic to measure the diameter of a méplat, therefore the biggest differences in a batch of cartridges can be noticed in the COAL measurements, which correspond not only to the seating depth, but to the differences in projectile geometry as well. This aspect indicates that to accurately estimate the seating depth influence on ballistic performance, it is necessary to measure the CBTO instead of COAL

when sorting the cartridges, to avoid variances in the projectile lengths itself.

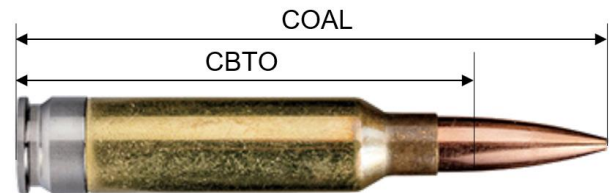


Fig. 1. COAL and CBTO of a small arms cartridge

In terms of ballistic performance, it is established that the bigger COAL/CBTO, the more volume inside the case, and therefore more propellant can be used, which provides higher muzzle velocity at lower pressures. Nevertheless, there are some restrictions in the maximum COAL, which are specifically important in the military solutions:

- bolt carrier group travel length – the maximum length of a cartridge is constrained by the distance that the bolt carrier group travels after each shot to extract the spent cartridge case from the chamber. If a cartridge exceeds this maximum COAL, it may interfere with the proper cycling of the weapon, potentially leading to failures in extracting and ejecting spent casings,
- magazine length – when considering a weapon system with magazine feeding, the maximum COAL will be restricted by the length of the magazine utilized. Assembling longer cartridges may cause malfunctions or even inability to use the rounds. In the case of different feeding methods, that issue is not a concern,
- elevated pressure – long cartridge assembly with a bullet positioned in direct contact with the barrel rifling while chambered, results in heightened resistance opposing the initial bullets movement. This leads to immediate opposition to the bullet's forward motion upon ignition due to the engraving force, thereby elevating chamber pressures to potentially hazardous levels. Seating the projectile a slight distance away (often referred to as a *bullet jump*) from the lands effectively mitigates this concern.

Due to the abovementioned, for user safety, the maximum COALs for each cartridge type are specified in the SAAMI and C.I.P regulations (CIP, 2024; SAAMI, 2015), as well as in separate military standards for military ammunition, for instance the 5.56x45 M193 (U.S. DoD, 1999).

Different ogive designs exhibit varying sensitivities to seating depth. Low-drag secant ogive projectiles, which offer the lowest drag coefficient and thus improved external performance, are considered more sensitive to seating depth than tangent ogive projectiles. A smooth juncture with the bearing surface facilitates self-alignment with the bore rifling, whereas an abrupt connection with the bearing surface leads to poor alignment with the rifling, and thus, greater sensitivity to seating depth. The combination of the aforementioned characteristics is found in hybrid ogives, where the bullet's nose profile is tangent up to the point of contact with the rifling and secant forward of that point.

Prior investigations (Thamna, 2018) have highlighted the importance of achieving uniform performance of cartridges, by improving the inspection process using an automatic visual inspection system to control the dimensions of each cartridge after assembly. The explained system provided an imperfections detection rate of 86.7% with a rate of 2 cartridges per second. Scientists (Li, 2022) utilized image processing to improve the assembly quality of the cartridge primer, which is a key part of the safety and reliability of ammunition. The general qualitative assessment of the influence of different COAL and CBTO in cartridge assembly was widely analyzed in the long-range shooting community, for instance by Berger Bullets (Litz, 2013), however, there is a need to quantify the effect of different seating depth on performance of diverse cartridge types, focusing on the different ogive profiles.

This study aims to assess the impact of the assembly variables within the context of different projectile designs, assessing their influence on ballistic performance, and focusing on the internal and external ballistics. By addressing those challenges the research seeks to enhance the understanding of the manufacturing process, aiming to assess the requirements of repeatability and precision of future small-arms ammunition production.

## 2. Material and methods

To systematically evaluate the impact of seating depth on ballistic performance – specifically focusing on muzzle velocity and shot dispersion at 50 meters, an extensive experimental framework was established. This section explains the methodological approach

adopted to investigate these parameters, detailing the laboratory setup and the specific characteristics of the cartridges utilized.

### 2.1. Ammunition

The authors precisely handloaded 30-06 Springfield cartridges using two types of projectiles, with various seating depths. With the use of the 30-06 cartridge cases (Sellier&Bellot), each cartridge was filled with RS60 propellant (ReloadSwiss), and large-rifle primer (Fiocchi). To analyze the considered parameters, especially the seating depth and the projectile's sensitivity to it in various configurations, the following projectiles were chosen for the experiment (Fig. 2):

- .30 Lapua Open Tip Match Scenar (10.85 g / 167 gr) GB422 – tangent ogive profile, bullet length:  $31.2 \pm 0.1$  mm, 3.74 g (57.7 gr) of RS60 propellant,
- .30 Lapua Open Tip Match Scenar-L (10.0 g / 155 gr) GB552 – secant ogive profile, bullet length:  $32.8 \pm 0.1$  mm, 3.72 g (57.4 gr) of RS60 propellant.

Both projectiles used in the experiment are Open-Tip Boat-Tail designs. Due to the beforementioned larger differences in the distance between the base of the bullet and its tip, than the base and the ogive, they were sorted by measuring each bullet's base to ogive distance.



**Fig. 2.** Bullets used for the experiment:  
Top: secant ogive profile Lapua Scenar-L,  
Bottom: tangent ogive profile Lapua Scenar

Followingly, each cartridge type was assembled with 5 different CBTOs using a single-stage reloading press, followed by dimension and weight control of each element and the whole cartridge assembly. The cartridge cases were primarily resized, trimmed, and cleaned to avoid any excessive influence on the cartridge's performance. The maximum difference in the CBTO distance was maintained at 1 mm, with a 0.25 mm difference between each configuration.

### 2.2. Experimental setup

The experiment was conducted in a 50-meter-long ballistic free-flight tunnel. The setup consisted of the following elements (Fig. 3):

- mobile firing stand STZA13M2 with universal ballistic breech UZ-2002 and velocity ballistic test 30-06 Springfield barrel with 1:10 inches twist, manufactured according to C.I.P. standard (Prototypa, Czech Rep.),
- muzzle velocity head EMG-1 (Prototypa, Czech Rep.),
- Phantom V2012 Ultra High-speed camera (Phantom, USA),
- light screen type 2521A at 5 m (Kistler, Switzerland),
- target system type 2523A at 50 m (Kistler, Switzerland).

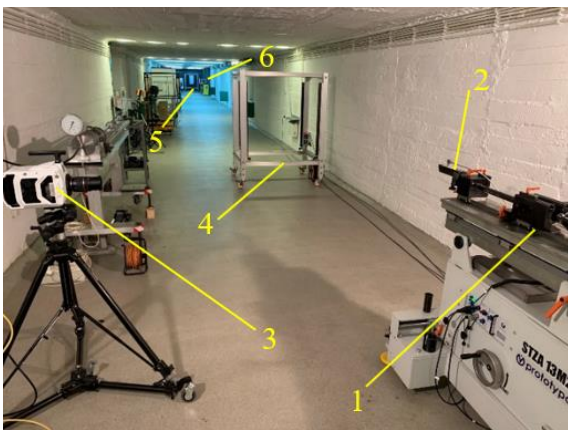


**Fig. 3.** Experimental setup  
 1 – STZA13M2, 2 – EMG-1, 3 – Phantom V2012,  
 4 – Kistler 2521A, 5 – Kistler 2523A, 6 – bullet trap

The measurements were performed with a series of shots for each specific CBTO of a given projectile type cartridge, measuring the muzzle velocity –  $V_0$ , velocity at 5 meters –  $V_5$ , coordinates, and velocity at the target at 50 meters –  $V_T$ . To analyze the bullet’s stabilization and initial yaw movement, the high-speed camera was used to record the initial bullet movement.

### 3. Results

Experimental data were examined individually for the different CBTOs of each projectile, to evaluate their sensitivity to seating depth changes. Firstly, to begin the analysis of shot dispersion, the stabilization of the bullets was confirmed. If a projectile is stable upon exiting the barrel, it remains stable throughout its entire trajectory up to the bullet trap at 50 meters (McCoy, 2009), hence, its behavior at the muzzle exit was analyzed. Both types of projectiles tested were found to be gyroscopically stable, characterized by

negligibly small yawing movement, therefore allowing the shot dispersion results to be considered reliable. An example of the bullet in motion at the muzzle exit is shown in Fig. 4.

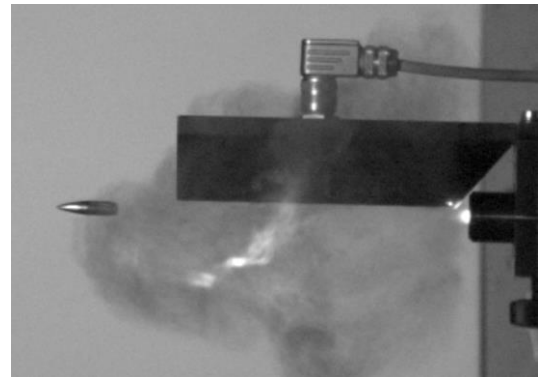


**Fig. 4.** Tangent projectile at the barrel muzzle

### 3.1. Tangent ogive projectile

The mean velocity at 5 m of shot groups of cartridges with tangent Lapua Scenar projectile varied from 933.2 m/s to 938.9 m/s with a maximum seating depth variation of 1.0 mm. The results are presented in Fig. 5 below.

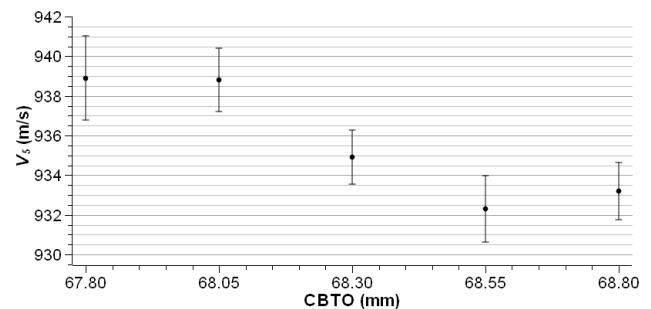


**Fig. 5.** Experimental results of velocity dependence on CBTO – tangent ogive profile

Following a procedure of 3 shots per each CBTO value, 5 groups of 3 shots were obtained with the same aiming point. To visually analyze the dispersion, the results are presented in Fig. 6.

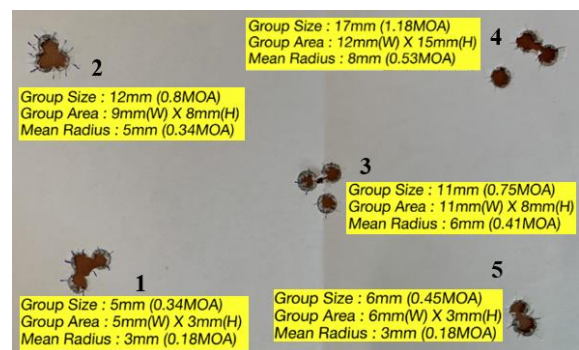


**Fig. 6.** Shot dispersion – tangent projectile

The shot dispersion differs significantly, depending on the CBTO, from a 3 mm mean radius in the case of group number 5, up to 8 mm for group number 4. In order to analyze the dispersion of shots regardless of the distance to the target, the mean radius was presented in minutes of angle – MOA. The average radius for the tangent projectile was estimated at 0.34 MOA, which equals 9.89, 19.78, and 29.67 mm at 100, 200, and 300 meters respectively. For each group, the dispersion analysis was performed, and the results are presented in Tab. 1.

**Table 1.** Experimental results of the tangent ogive projectile cartridges

No	CBTO (mm)	Mean $V_5$ (m/s)	Group size (mm)	Mean Radius (mm)	Mean Radius (MOA)
1	68.80	932.3	5	3	0.18
2	68.55	933.2	12	5	0.34
3	68.30	934.9	11	6	0.41
4	68.05	938.8	17	8	0.53
5	67.80	938.9	6	3	0.18
AVG			10.2	5.0	0.34

### 3.2. Secant ogive projectile

The mean muzzle velocity of shot groups of cartridges with secant Lapua Scenar-L projectile varied from 935.5 m/s to 949.7 m/s with a maximum seating depth variation of 1.0 mm. The results are presented in Fig. 7 below.

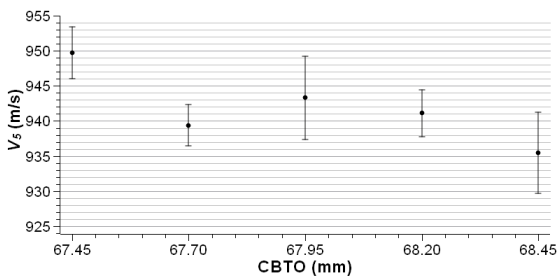


**Fig. 7.** Experimental results of muzzle velocity dependence on CBTO variance – secant ogive profile

The results of shot groupings indicate slightly stronger correlation between the seating depth and external ballistics of the bullets. The results are shown in Fig. 8.

In the case of the secant ogive projectile, the lowest mean radius of 4 mm was achieved with group number 3, and the highest – 6 mm for groups 4 and 5. The average mean radius estimated for the 5 groups equals 0.36 MOA, which gives 10.47, 20.94, and 31.41 mm for 100, 200, and 300 meters. The results of the shot dispersion analysis are presented in Tab. 2. The mean

radius and group sizes are noticeably higher for the secant profile projectile cartridges.

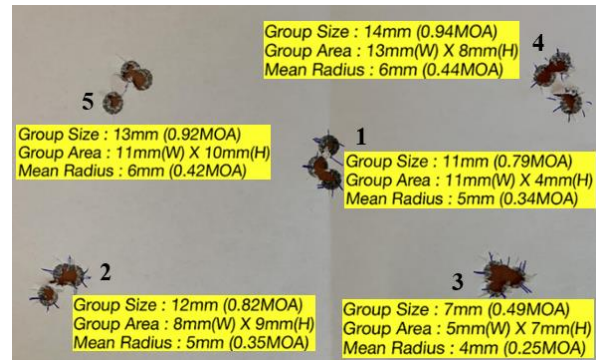


**Fig. 8.** Shot dispersion – secant projectile

**Table 2.** Experimental results of the secant ogive projectile cartridges

No	CBTO (mm)	Mean $V_5$ (m/s)	Group size (mm)	Mean Radius (mm)	Mean Radius (MOA)
1	68.45	935.5	11	5	0.34
2	68.20	941.1	12	5	0.35
3	67.95	943.3	7	4	0.25
4	67.70	939.4	14	6	0.44
5	67.45	949.7	13	6	0.42
AVG			11.4	5.2	0.36

### 3.3. Geometry analysis of military cartridges

To evaluate the impact of variations in CBTO within a batch on the performance of the rounds, an analysis was conducted on the geometry of military-use 7.62x51 mm Ball cartridges. The findings from 21 measurements suggest that the CBTO in a batch, and consequently the seating depth, can vary by as much as 0.48 mm. Given this variability, conducting an analysis with a CBTO difference of 1 mm for a .30 projectile is justified to determine the significance of precise seating depth inspections in the production of military ammunition.

## 4. Discussion

To analyze the results and formulate conclusions, it is necessary to consider the following aspects of the performed analysis:

- measurements of projectile geometries included verifying the COAL, CBTO, the diameter, and the weight of each projectile. Variations in ogive shape and méplat diameter are supposed to be negligible, therefore were not taken into account,
- variability in internal ballistics performance may occur from one cartridge to another due to inconsistent propellant powder filling, even

when the CBTO is consistent. These differences are expected to be significantly smaller than those caused by changes in CBTO,

- despite the thorough preparation of the cartridge cases before ammunition assembly, there is a certain influence noticeable on the performance of prepared cartridges. Variations in internal and external dimensions between each case led to differences in muzzle velocities among shots within the same CBTO groups,
- the tests were conducted on a small sample which is a simplification of the whole population, therefore the probability error must be considered while analyzing the results,
- the measurement system accuracy must be considered, especially concerning the measured velocities of the projectiles.

The findings indicate that the cartridges with secant ogive profile projectiles experienced greater muzzle velocity spread when the seating depth of the bullet varied, with a difference of mean velocities reaching up to 14.5 m/s, in contrast to 6.6 m/s observed in tangent profile projectiles.

Although muzzle velocity did not directly correlate with shot dispersion at the target, the mean radius equals 5.0 mm for the tangent projectile cartridge and it is slightly higher – 5.2 mm, for the secant bullet. The group size is also larger for the secant projectile configuration when compared to the tangent projectile – 11.4 mm versus 10.2 mm. While these differences in the mean radius are relatively minor at 50 meters, they increase with target distance, potentially exceeding 30 mm for secant projectiles at 300 meters due to inconsistencies in CBTO and thus seating depth.

The results indicate that a tangent ogive profile reduces the sensibility of a cartridge on seating depth variations, though it is characterized by a higher drag. The balance between drag and seating depth sensitivity should be thoroughly examined in further detail.

Dimensional analysis of a batch of 7.62x51 mm Ball military-use rounds indicated that the maximum CBTO variation within a batch could reach 0.48 mm. Given the analysis results, where the maximum CBTO differences were up to 1 mm, the impact of these variations in seating depth on cartridge performance should be considered.

## 5. Conclusions

Bearing in mind the abovementioned, the following conclusions can be drawn:

- seating depth has a noticeable influence on the ballistic performance of a cartridge, by incre-

asing the muzzle velocity with the increase of the seating depth,

- cartridges with secant profile ogive projectiles are more sensitive to variations in the seating depth of the projectile compared to those with tangent profile projectiles,
- to achieve higher precision of small-arms ammunition, it is essential either to use higher drag, tangent profile projectiles or to ensure high repeatability in the seating depth of bullets in the cases,
- the effect of the seating depth may become imperceptible due to imperfections and variations in geometries of the cartridge cases, primers, and the associated differing characteristics of the process of propellant combustion,
- military ammunition may experience a high variation of the shot dispersion at the target due to seating depth inconsistencies.

The results have strong implications for future ammunition design by providing a resource in the analysis of the balance between manufacturing low drag coefficient bullets while maintaining high precision. Further works should focus on analyzing the hybrid ogive projectiles' external ballistics performance with the use of both CFD simulations and live firing, as well as on analyzing the bullet's performance dependence on minor damage caused during production and assembly, which may cause irregularities and asymmetries in the geometry.

## Acknowledgments

The work was supported by the Warsaw Military University of Technology (Poland) within the UGB 22 741 grant funds.

## References

- Commission Internationale permanente pour l'épreuve des armes à feu portatives, *TDCC - TABLES OF DIMENSIONS OF CARTRIDGES AND CHAMBERS*. Retrieved 12.04.2024 from [https://bobb.cip-bobb.org/en/tdcc\\_public](https://bobb.cip-bobb.org/en/tdcc_public).
- Frost G. (1990). *Ammunition making*. Washington, D.C.: National Rifle Association.
- Li C., Wang C., Liu P., Zhao Y. & Zhao J. (2022). Research on quality improvement of bullet Assembly based on image Processing. *28th International Conference on Mechatronics and Machine Vision in Practice 2022*. 1-4.
- Litz B. (2013). *Effects of Cartridge Over All Length (COAL) and Cartridge Base To Ogive (CBTO)*. USA: Berger Bullets. 148-158.
- McCoy R. (2009). *Modern Exterior Ballistics - The Launch and Flight Dynamics of Symmetric Projectiles 2nd ed.* Atglen: Schiffer Military History.



SAAMI. (2015). *Voluntary Industry Performance Standards for Pressure and Velocity of Centerfire Rifle Ammunition for the Use of Commercial Manufacturers*, Newtown, U.S.

Thamna, A., Srisungsithisunti, P. & Dechjarem S. (2018). Real-Time Visual Inspection and Rejection Machine for

Bullet Production, *ICEI* 2018. 13–17. 10.1109/ICEI18.2018.8448641.

U.S. DoD. (1999). *MIL-C-9963F Military specification: Cartridge, 5.56mm, Ball, M193*. U.S: Department of Defense.

## CLASSIFICATION GRAPH OF POKA-YOKE TECHNIQUES FOR INDUSTRIAL APPLICATIONS: ASSEMBLY PROCESS CASE STUDIES EFFECTIVENESS EVALUATION

### GRAF KLASYFIKACJI TECHNIK POKA-YOKE DO ZASTOSOWAŃ PRZEMYSŁOWYCH: OCENA EFEKTYWNOŚCI STUDIÓW PRZYPADKÓW DLA PROCESU MONTAŻU

Dorota STADNICKA<sup>1,\*</sup> , Dario ANTONELLI<sup>2</sup> 

<sup>1</sup> Faculty of Mechanical Engineering and Aeronautics, Rzeszów University of Technology, Al. Powstanców Warszawy 12, Rzeszów, Poland

<sup>2</sup> Department of Production Systems and Economics, Politecnico di Torino, Corso Duca degli Abruzzi 24, I 10129 Torino, Italy

\* Corresponding author: [dorota.stadnicka@prz.edu.pl](mailto:dorota.stadnicka@prz.edu.pl)

#### Abstract

It is widely acknowledged that the expenses associated with substandard quality constitute a significant portion of a company's overall costs. Consequently, organizations adopt quality management systems and implement corrective and preventive measures to reduce these expenses. Within these implementations, Poka-Yoke (P-Y) techniques are notably prominent. Theoretically, these techniques are designed to prevent mistakes that lead to costs, especially quality-related costs associated with nonconforming products. This study proposes a classification graph of P-Y techniques, which serves as a tool for evaluating the effectiveness of these techniques in preventing errors that lead to product nonconformities, machine failures, operator injuries, or environmental threats. The Classification Graph was developed based on a study of 139 P-Y solutions implemented in 24 companies operating in the automotive, aviation, and metal processing industries. The value of this graph lies in its ability to easily evaluate and prioritize different P-Y techniques, aiding in the design of new techniques and the improvement of existing ones to enhance the reliability of production systems.

**Keywords:** mistake proofing, Poka-Yoke, effectiveness, collaborative robots, assembly

#### Streszczenie

Powszechnie uznaje się, że wydatki związane z jakością poniżej standardu stanowią znaczną część ogólnych kosztów firmy. W związku z tym organizacje przyjmują systemy zarządzania jakością i wdrażają środki korygujące i zapobiegawcze w celu zmniejszenia tych wydatków. W ramach tych wdrożeń techniki Poka-Yoke (P-Y) są szczególnie ważne. Teoretycznie techniki te mają na celu zapobieganie błędom, które prowadzą do kosztów, zwłaszcza kosztów związanych z wyrobami niezgodnymi. W niniejszym badaniu zaproponowano wykres klasyfikacji technik P-Y, który służy jako narzędzie do oceny skuteczności tych technik w zapobieganiu błędom, które prowadzą do niezgodności wyrobów, awarii maszyn, obrażeń operatorów lub zagrożeń dla środowiska. Graf klasyfikacji został opracowany na podstawie badania 139 rozwiązań P-Y wdrożonych w 24 firmach działających w branży motoryzacyjnej, lotniczej i obróbki metali. Wartość tego wykresu polega na jego zdolności do łatwej oceny i ustalania priorytetów różnych technik P-Y, co pomaga w projektowaniu nowych technik i ulepszaniu istniejących w celu zwiększenia niezawodności systemów produkcyjnych.

**Słowa kluczowe:** zabezpieczenie przed błędami, Poka-Yoke, efektywność, roboty współpracujące, montaż

## 1. Introduction

In order to ensure that a company remains on the market, it must be competitive in terms of product quality and selling price. That is why, it has to find strategies to reduce costs while preserving the level of quality expected by their customers.

It has been noticed that a considerable part of companies' costs are costs of poor quality (Tkaczyk and Jagła, 2001). For this reason, the companies began to undertake the activities concerning cost minimization (Yoo et al., 2012). To find a source cause of the quality problems the companies undertake various actions. They use simple quality management tools, such as Ishikawa diagram (Kumar et al., 2009) or methods such as FMEA (Pinosova and Andrejiova, 2023; Xiuxu, 2011; Sellappan and Palanikumar, 2013) to find possibilities for improvements. Additionally, more and more popular is six sigma methodology, which is applicable for more difficult quality problems (Valles et al., 2009; Yusuf and Halim, 2023). The result of these analyses is an information about weak points in production system, where any corrective and preventive actions should be undertaken.

However, it is not solely about enhancing control processes to prevent nonconforming products from reaching customers. First of all, it is about undertaking preventive actions to prevent the production of nonconforming products, for example by using control charts (Chen et al., 2011; Dahari et al., 2025). That is why, different kinds of solutions, which can prevent nonconformities or which can significantly minimize their number, are implemented. These solutions are called Poka-Yoke (fail safe) and they are implemented not only in the production companies (Martinelli et al., 2022; Kozikowski et al., 2022; Trojanowska et al., 2023) but also in services (de Saint Maurice et al., 2011; Amaral et al., 2023). Literature propose not only physical but also digital Poka-Yoke techniques (Rahardjo et al., 2023). Various Industry 4.0 technologies can serve as Poka-Yoke (P-Y) solutions (Lucantoni, et al., 2022). Since Industry 4.0 technologies support the achievement of sustainable development goals, as highlighted in (Mabkhot et al., 2021), it can be concluded that the use of P-Y solutions based on these technologies also has a positive impact on the sustainable development of enterprises. Among others the following technologies can be found in P-Y: augmented reality (Andersen et al., 2009; Chimienti et al., 2010; Azuma et al., 2012), virtual reality (Yin et al., 2017;), Internet of Things (Ramadan and Salah, 2019), wireless technologies (Gładysz and Buczacki, 2018), real time data analysis (Garza and Das, 2001), Big Data Analysis (Muharam and

Latif, 2019), mobile technologies (Grout, 2007; Hakkarainen et al., 2008), fuzzy logic (Al-Araidah et al., 2010), and others.

The aim of this paper is to propose a classification table and an evaluation tool supporting the adoption of P-Y techniques that take into account not only product defects, but above all, mistakes resulting in the creation of nonconforming products, as well as mistakes affecting the employee, the production system and the environment. The construction of the tool begins with the classification of possible P-Y techniques to then build a Classification Graph that will support the assessment of the effectiveness of P-Y techniques in relation to specific process conditions encountered in the industrial environment.

The next section of this paper reviews the definition of P-Y. Subsequent to this, the following section describes the methodology used to create a classification for P-Y techniques, along with the proposed Classification Graph. The application is then demonstrated by assessing three distinct P-Y techniques. The final section provides a summary and emphasizes the need for further research in this area.

## 2. Poka-Yoke definitions

In literature many definitions of P-Y are present. The review of these definitions is shown in **Table 1**. According to some authors, P-Y is a technique which prevents mistakes or, according to others, it is a solution which allows to discover and correct the mistakes that have already occurred.

Other definitions state that these are the solutions which should prevent not the mistakes but their outcomes. Different definitions probably derive from the fact that there are different kinds of P-Y techniques as well as different applications of the same solution.

For example, in the work (Hollnagel, 2004), for the application in IT the author divides P-Y techniques into three types:

- Physical solutions which block the flow of mass, energy or information, and do not depend on the users' interpretation of them (e.g. a wall);
- Functional solutions which might be switched on and off depending on the situation (e.g. a lock or a password), independently from the user's interpretation;
- Symbolic solutions which if require interpretation, appear physically at the moment they are needed (e.g. a safety sign).

**Table 1.** Poka-Yoke definitions

Definition	References
A mechanism for detecting errors and defects, which inspects 100% of the items, working independently from the operator's attention span	(Shingo, 1988)
A device used to prevent the defect from occurring in a machine or in a process	(Joseph et al., 1996)
A mechanism for detecting, eliminating and correcting errors at their source, before they reach the customer	(Plonka, 1997)
Devices the process is equipped with to prevent the special causes that result in defects, or to inexpensively inspect each item that is produced to determine whether it is acceptable or defective	(Tsou et al., 2008)
The Poka-yoke technique identifies human errors and creates ways to eliminate them, however, it depends on the occurrence of an error in order to prevent its future occurrences. It is any mechanism within a lean manufacturing process that helps an equipment operator to avoid mistakes.	(Lopes et al., 2013)
The systematic practice of eradicating errors by locating their root cause	(Middleton, 2001)
A quality improvement methodology to prevent mistakes from in order to minimize the negative consequences	(Krajewski et al., 2007)
A poka-yoke is the use of a process or design features to prevent errors or the negative impact of errors	(Grout, 2007)
A device that either prevents or detects abnormalities, which might be detrimental either to the product quality or to the employees' safety	(Saurin et al., 2012)
Automatic devices or methods to detect problems before or as they occur using a Poka-Yoke device to minimize the negative consequences	(Al-Araidah et al., 2010)

S. Shingo divided Poka-Yoke techniques according to the goals they have to accomplish in a quality system (Shingo, 1988):

- Source inspection, called proactive Poka-Yoke devices, realized to avoid the occurrence of a defect;
- Self-inspection to detect a defect in the operation in which the defect is generated;
- Successive inspection which detects a defect in the operation that follows the operation in which it was generated;
- Judgment inspection which detects a defect a few operations ahead of the one in which it was generated.

In industry, Zero Quality Control (ZQC) Poka-Yoke takes a variety of forms such as (Evans, 2005):

- 100% inspection;
- Identifying defects as close to the defect source as possible;

- Taking corrective actions concerning a defect in order to avoid the reoccurrence of that defect in the future;
- Designing the processes in order to avoid defects.

In the work (Lazarevic et al., 2019) the authors based on a literature review distinguished the following types of P-Y devices:

- Passive devices P-Y;
- Active preventive P-Y;
- Active, for detection P-Y;
- Hybrid active, preventive;
- Hybrid active, detection.

The presented definitions are useful for classification purposes but focus mostly on product defects which are the consequences of mistakes. While a new approach proposed in this paper focuses on mistakes avoidance. In light of this, a new definition is proposed aimed at supporting the evaluation of P-Y techniques' effectiveness in preventing or detecting various mistakes impacting both, the product and the production process.

In present study, the following definition of P-Y is proposed: *Poka-Yoke is a solution developed to reduce or completely eliminate mistakes that can lead to product nonconformities, machine failures, operator injuries, or environmental threats.*

### 3. Poka-Yoke classification

Poka-Yoke techniques can be classified according to a number of different criteria. In the work (Saurin et al., 2012) a method for the evaluation of P-Y techniques is proposed. This method is relatively detailed and includes many evaluation criteria. Thus, the question arises if companies are willing to use the method in everyday practice. In the work (Antonelli and Stadnicka, 2016) the Fuzzy Inference methodology is proposed to assess the P-Y solutions. However, especially for SMEs, a less complex method could be recommended.

In this work a straightforward method for the assessment of P-Y techniques is proposed. To allow the application of the method already in the design phase, i.e. before having any quantitative data on the number and type of defects in production, binary evaluation criteria based on the presence or absence of specific characteristics were used.

To propose a classification of P-Y techniques a research in industry was performed. 139 P-Y solutions from 24 companies operating as suppliers in automotive, aviation and metal processing industry were investigated. The analysed P-Y use such technologies as cameras, machine vision, augmented reality, sensors, automation, big data analytics, real-time data

processing, barcodes, visualisation, vibrofeeder, and others. The companies were chosen among those that presented their solutions at meetings dedicated to lean manufacturing. P-Y techniques were identified based on industrial expertise and knowledge, and the inclusion criteria were not based on preliminary evaluations.

Figure 1 shows structure of investigated companies and number of studied P-Y techniques. On the base of gathered information a Classification Graph of P-Y solutions is developed (Figure 2). The Classification Graph can help with evaluation of effectiveness level of P-Y solutions.

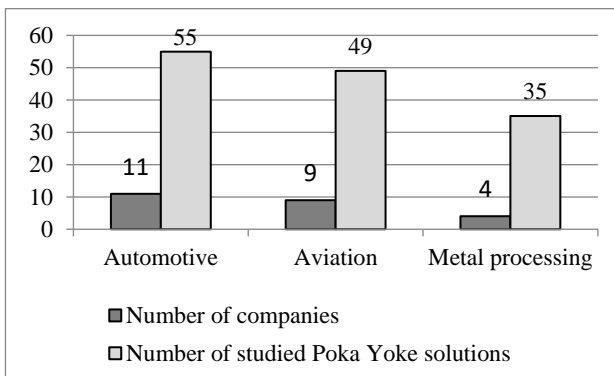


Fig. 1. Investigated companies and Poka-Yoke solutions

During the study of P-Y techniques, the following analyses were conducted:

- Analysis of work performed at a specific workstation, where an operator might make a mistake;

- Analysis of mistakes that were made or could potentially be made;
- Analysis of the consequences of mistakes that occurred or could potentially occur;
- Analysis of existing and proposed P-Y solutions to implement.

Table 2 presents a classification of P-Y solutions summarizing whether the solution prevent mistakes or not. The mistakes may lead to nonconforming products. By implementation of P-Y techniques it is possible to prevent mistakes or to identify mistakes before it leads to production of a nonconforming products. P-Y which are able to discover mistakes very fast will prevent nonconformities but will not prevent time waste and related costs. Therefore, in this study focus is put on preventing mistakes. Figure 2 presents a graph for the prioritizing of P-Y techniques. In general, there are P-Y techniques that can be very highly effective and others that can have very low effectiveness.

Certainly, it should be clearly underlined that, even if quality control is performed on the entire production, it is impossible to assure the absence of defects. It stems from the fact that none of the systems is absolutely reliable. Failures, fluctuation in power supply, hidden material defects can always emerge in technical devices which are designed to control and monitor a process.

Table 2. Classification of Poka-Yoke techniques

Type of Poka-Yoke	Function	Task	Goal	Effectiveness in mistake proofing
Technical devices	Preventive	Preventing mistakes	Zero mistakes	High
	Corrective	Stopping the process in case of a mistake	Preventing the flow of nonconforming products to the next step of the process	No mistake proofing
	Informative and preventive	Transferring the information concerning the probability of making a mistake	Preventing mistakes	Medium
	Warning	Transferring the information on a mistake made	Disclosing a place for improvement	No mistake proofing
Organizational solutions	Informative	Transferring the information on the proper way to perform a process in order to avoid mistakes	Preventing mistakes	Low
	Corrective	Transferring the information on what to do in case of making a mistake	Preventing reoccurrence of mistakes	No mistake proofing

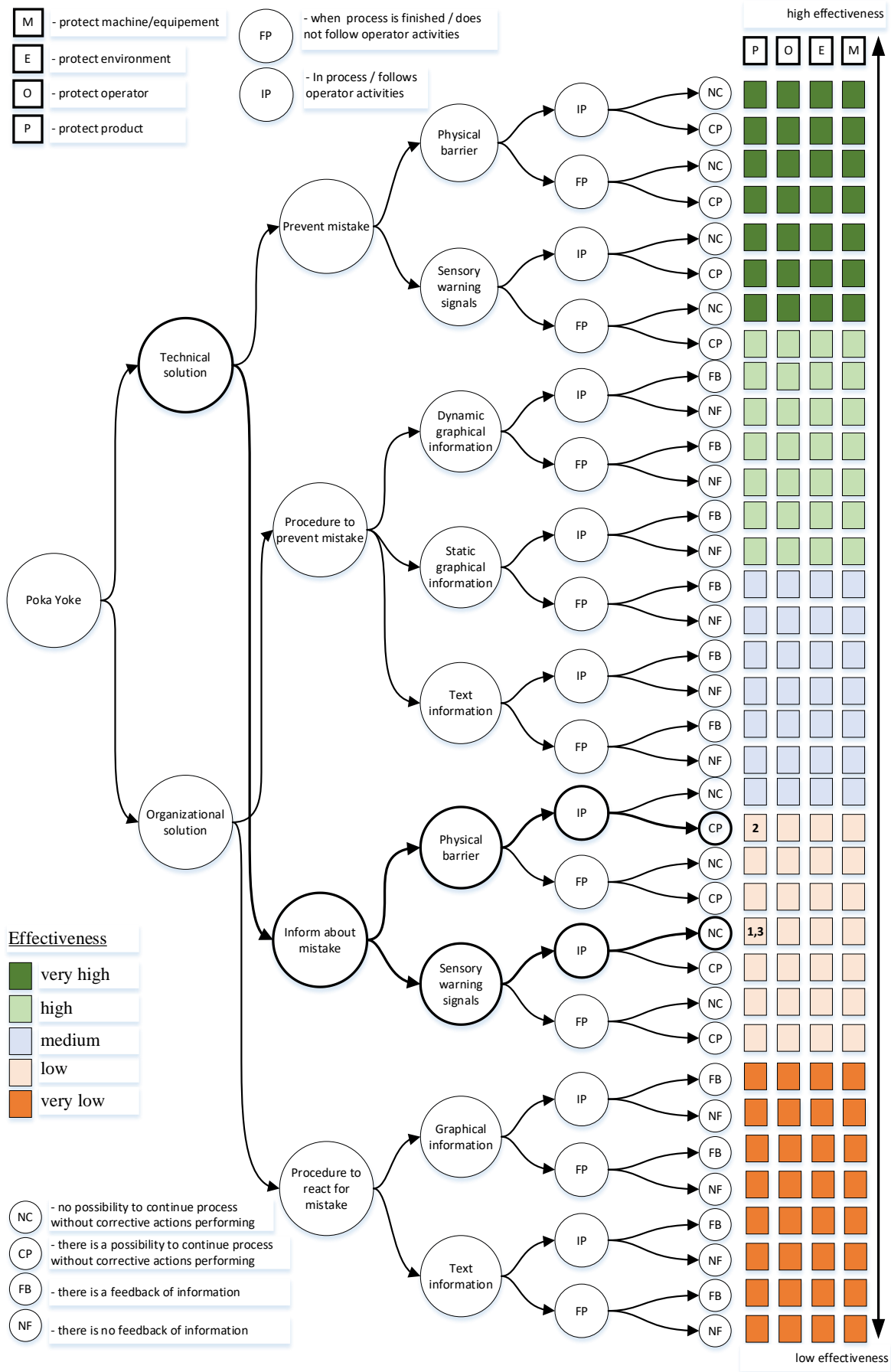


Fig. 2. Classification graph of Poka-Yoke techniques

Lacking a control group, i.e. a set of pieces that are produced without using P-Y, it is not always possible to give a quantitative evaluation of P-Y effectiveness in terms of number of defects avoided.

To place a given P-Y technique on the graph in Fig. 2 it is necessary to make a series of binary or choices: the solution is technical or organisational; is preventive or corrective, it operates through a barrier or through signals; information is given through graphic or textual outputs; P-Y operates during the process or at the end.

We assume that technical devices will have higher efficiency, particularly if a physical barrier is put in place. This barrier will physically prevent mistakes in a process as well as it will stop a process from continuing unless the corrective actions are implemented. In some of the solutions it is possible for an operator to decide if a process is to be continued howsoever without corrective actions. However, such a solution has already lower effectiveness because it depends on a subjective employee's decision (Stewart et al., 2001).

Despite that fact, this solution is attributed with a high level of efficiency assuming that the employees are well prepared for their work. Physical solutions, which warn an operator about the possibility of making a mistake by a sound, vibration or light signal (sensory warning signals), are less effective. However, they also require an adequate operator's reaction before the mistake appears in a process, or before the failure appears in a product.

Further, there are also less effective P-Y techniques which only inform about mistakes that have been made. However, they still allow for a quick reaction and, thanks to that, they reduce nonconformities costs, which can appear in relation to the mistake or which have already appeared. Theoretically, these solutions shouldn't allow, in spite of the mistakes already made, the negative consequences of them. Another group of P-Y technique includes organizational solutions, which exist in the form of procedures prepared for certain processes. Depending on the form of the procedure and the way of information transmission to an operator during the process, the solutions can have different effectiveness. In the proposed classification model, a dynamic and a static way of transmitting the graphical information are taken into consideration. The information can also take the form of a text. The procedures can concern activities which should be done to prevent mistakes or activities which should be done in case a mistake has already been made. It is worth to emphasize that when the information is transmitted successively and follows the process, the solution is more effective. Finally, it is also essential whether the information

takes into consideration the actual state of a process, or whether it is independent from what has really been done in the process.

P-Y techniques, which should prevent mistakes in a process or reduce the consequences of mistakes made, should simultaneously protect a product against defects. The proposed method recommends to assess additionally if the P-Y techniques protects a product, an operator, a machine and/or the natural environment against the consequences of mistakes made in the process by an operator.

In the following sections some examples of P-Y techniques are presented, classified and evaluated. The results of this can be seen on the Classification Graph (**Figure 2**) where the numbers (1, 2, 3) representing the analysed case studies have been placed.

For evaluating effectiveness, a 5-level Likert scale was adopted associated to corresponding effectiveness classes: very low for no error prevention, low for information, medium for error identification, high for error identification before it results in a non-compliant product, and very high for error prevention.

## 4. Case study 1: Kitting process

### 4.1. Process description

Kitting process of assembly sets is realized manually by operators (Wyskiel, 2014). Elements for kitting are taken from containers and placed into a box. A label, which specifies the contents of the box, is then affixed to it. Each set consists of several elements, making it easy for the operator to make a mistake during the kitting process.

### 4.2. Poka-Yoke technique description

The work procedure for the workstation equipped with a P-Y solution is as follows:

The computer screen displays a production order containing information about what should be packed in the assembly set. The worker picks the first item from the list and scans its barcode using a barcode reader. The scanned item is then placed into a box. The list updates to confirm that the correct item has been selected. If an incorrect item is taken, a notification will appear on the screen. Once all items are packed, the operator can print a label. This label is then affixed to the box.

The solution presented in **Figure 3** is a technical system that alerts the operator of a mistake when an incorrect item is selected for packing. The operator receives a sound signal and sees a notification on the screen. This alert occurs during the packing process, allowing the operator to rectify the mistake immediately. This means the operator can then select the correct item and pack it, ensuring that

the box contains all the necessary elements for assembly.

The system prevents the operator from continuing the process until all necessary barcodes for the set have been scanned.



**Fig. 3.** Workstation for kitting

Only after scanning can a label be printed and the production order closed. This solution safeguards the product against non-conformities but does not prevent operator mistakes.

#### 4.3. Poka-Yoke classification and evaluation

This is a technical solution designed to mitigate mistakes in kitting processes. While it does not prevent mistakes entirely, it informs the operator when a mistake occurs, such as selecting the wrong component. Although the system cannot prevent the addition of incorrect or extra elements into a box, it ensures that all necessary components are included, thereby preventing the escalation of mistake consequences. On the computer screen, graphical information is displayed along with a sound signal when a mistake is detected during the process, not afterward. The process cannot continue until corrective actions are taken; this means the operator must select and scan the correct item, which is then placed in the box. This solution is aimed at preventing the preparation of non-conforming sets. It does not address operator safety, environmental protection, or machine safeguarding.

The analysis clearly indicates that to enhance the solution, an improvement should be implemented during the handling phase to prevent the operator from selecting the wrong component. This would involve installing a device that automatically discards a part into a discharge bucket if the scanner detects an incorrect barcode. There are several methods for implementing this type of device. Although this improvement does not prevent the mistake itself, it mitigates the consequences of the mistake in the final kitting process. According to the proposed methodology, the effectiveness of this solution is considered to be low.

## 5. Case study 2: System of laser inspection of rolling bearings' seals assembly

### 5.1. Process description

A laser inspection system for seals in rolling bearings has been implemented on the production line (Czajka et al., 2010). This line conducts the assembly process using automated control equipment, which operates without direct human intervention (see **Figure 4**).

The seals are transferred from a storage bin and correctly positioned on a bearing by being pushed into place using a manipulator.

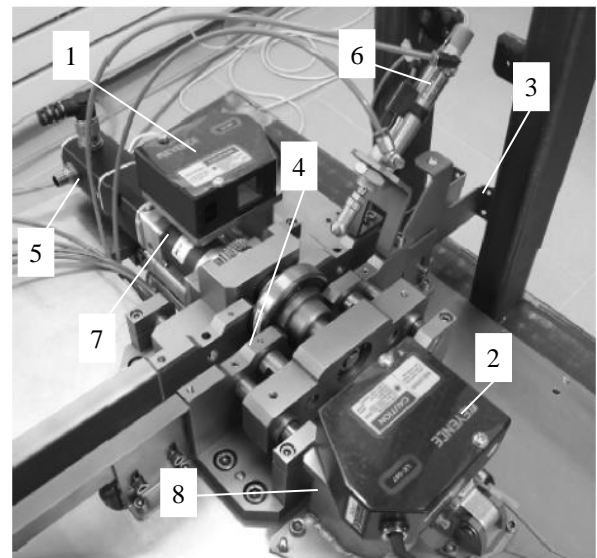


**Fig. 4.** Control unit: 1, 2 – laser head, 3 – chute, 4 – setting with a bearing in measurement position, 5 – electric drive of bearing rotation, 6 – pneumatic basic elements, 7, 8 – pneumatic drives

### 5.2. Poka-Yoke technique description

During the process, the following defects in seals can occur (Czajka et al., 2010):

- Absence of a seal in a bearing;
- Seal placed inversely;
- Seal improperly positioned relative to the bearing dimensions;
- Surface of the seal is folded.

These defects are identified by a laser control system. A photo of the control unit is shown in **Figure 4**. Bearings that exhibit any of these defects are segregated from the acceptable ones and classified as nonconforming products.

However, the process continues without immediate corrective actions to address the underlying causes of these defects.



### 5.3. Poka-Yoke classification and evaluation

The system described is a technical solution that identifies errors in the seal assembly process by using a physical barrier. This barrier prevents nonconforming products from advancing to the next stage of the production process by automatically removing them. Despite this, the assembly process itself is not halted; instead, the control system continues to operate, merely ensuring that flawed products are excluded.

This technical solution does not prevent errors; it merely signals when an error has occurred, specifically identifying seals that are improperly affixed to bearings. The physical barrier ensures that these defective products do not proceed further in the production line. The process continues without interruption, and no immediate corrective actions are taken to address the root cause of the defects. The primary goal of this system is to remove bearings with incorrectly assembled seals from the production line. According to the proposed methodology, this solution is considered to have low effectiveness.

## 6. Case study 3: Manual Assembly Processes Using Real-Time Image Detection

### 6.1. Process description

Manual assembly operations in manufacturing are often susceptible to human error, particularly in tasks involving complex sequences or a large number of components. This case study investigates the integration of a pre-trained YOLO (You Only Look Once) image detection model into a factory assembly workflow to provide real-time feedback on part sequencing, aiming to mitigate errors. The YOLO model utilizes computer vision techniques to rapidly analyse a live video feed of the assembly workspace. It compares the current state against a reference database of correct assembly steps. If a part is placed out of sequence, the system generates an immediate visual alert, notifying the worker of the deviation. This report details the YOLO model's architecture, the training process, its integration into the assembly station, and a quantitative assessment of its impact on error rates and assembly efficiency.

### 6.2. Poka-Yoke technique description

This case study explores a collaborative human-robot assembly strategy, assigning sub-tasks to optimize efficiency and accuracy. The system leverages the strengths of both humans and robots: the robot performs object detection and sequence checks, while the human collaborator handles workpiece manipulation and judges the robot's recognition. This

approach facilitates mutual learning – the robot alerts the human operator to placement errors, and the human provides feedback on the robot's object recognition, enabling continuous improvement within the system.

A collaborative assembly operation is performed using an OMRON TM5-900 robot equipped with two distinct camera systems. The robot's integrated 5 Mpx autofocus camera (100mm-∞) facilitates precise positioning. An additional top-mounted camera handles primary object detection tasks (see **Figure 5**).

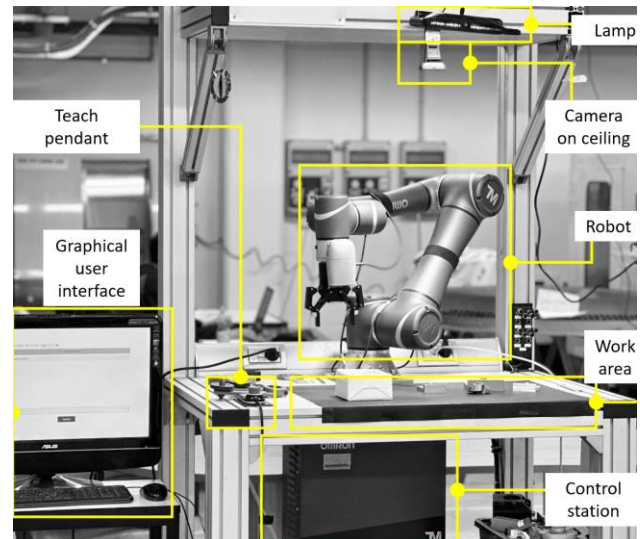


Fig. 5. Workstation

Object recognition is implemented as a pattern recognition problem, utilizing the YOLOv7 deep learning algorithm for classification. YOLOv7's efficient single neural network architecture divides input images into grids, with each cell detecting and classifying objects within its region. Anchor boxes further enhance its accuracy.

YOLO (You Only Look Once) is a highly popular and efficient real-time object detection algorithm. Unlike previous approaches that repurposed image classifiers, YOLO uses a single convolutional neural network (CNN) to perform detection in one pass. This makes it remarkably fast and suitable for real-time applications.

For training, images were resized to 640x640 pixels with a batch size of 16. After 300 epochs, the model achieved an accuracy of 96.7% and a recall of 100%. First, the system establishes the correct assembly sequence: "4 holes, 3 holes, 2 holes, 4 holes square".

The assembly task begins. The worker picks up a part and places it on the designated platform. The camera detects the part type and verifies its position in the sequence.

Possible System Responses are as follow (**Figure 6**):

- Correct Part, Correct Sequence: "Correct part and sequence".
- Correct Part, Wrong Sequence: "Wrong sequence. Please place: (name of next part)".
- Wrong Part: "Wrong part. Please place: (name of correct first part)".

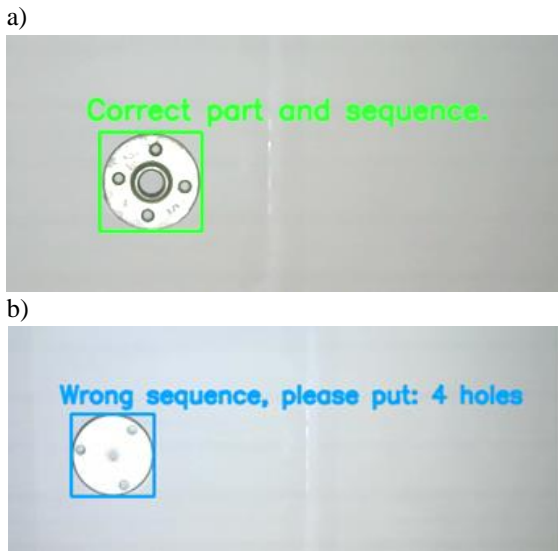


**Fig. 6.** Two kind of results for part and sequence detection: (a) object is in the list and in the right sequence; (b) object is in the list but in the wrong order

### 6.3. Classification of the solution

The assembly task begins. The worker picks up a part and places it on the designated platform. The camera detects the part type and verifies its position in the sequence. To summarize:

- The solution is technical – camera is applied to identify the objects;
- Inform about mistakes – when the wrong object is taken by an operator the system informs the operator about the mistake;
- Sonic or light signal – an information will be passed to the operator as voice information;
- In process / follows operator activities – the camera follows operator movements while realizing the process;
- There is no possibility to continue process without corrective actions performing – the software blocks information related to the assembly process step so the operator will not know what to do next before the correct object will be placed in the assembly area;
- The solution protects against the production of a nonconforming product.

From the classification graph it can be seen that this P-Y technique has not so high effectiveness. The

solution prevents from production of a nonconforming product but does not prevent from mistakes. It means that operator can make mistake and take wrong component but this will be discovered immediately and the wrong component will not be used in the assembly process. Only time wastes will appear because the operator will have to put down the wrong component and pick up another.

The solution could be more effective if a technical solution or even procedure to prevent mistakes would be implemented in such way that the operator has no possibility to take a wrong part.

## 7. Discussion

The Classification Graph, as proposed, offers a simplified yet effective approach to evaluating P-Y techniques, particularly beneficial for small and medium-sized enterprises (SMEs) with limited resources. By focusing on objective characteristics and avoiding complex mathematical calculations, the Graph enables a rapid assessment of existing P-Y solutions and provides insights for their improvement. This streamlined evaluation process can lead to substantial cost savings by identifying and rectifying ineffective or inefficient P-Y implementations.

In terms of cost-effectiveness, the Classification Graph aids in prioritizing P-Y techniques based on their potential impact on error reduction and overall process improvement. By identifying high-impact areas for intervention, companies can allocate resources more efficiently, focusing on implementing or enhancing P-Y solutions that offer the greatest return on investment. This targeted approach not only minimizes costs but also maximizes the effectiveness of P-Y implementation, leading to improved quality, reduced waste, and increased productivity.

Furthermore, the Classification Graph indirectly contributes to sustainability efforts. By promoting error prevention and reduction, P-Y techniques inherently support resource conservation and waste minimization. For instance, preventing defects in the assembly process reduces the need for rework, scrap, and additional material consumption. Additionally, P-Y solutions that focus on operator safety and environmental protection directly align with sustainability goals by minimizing the risk of accidents, injuries, and environmental damage.

The case studies presented in this paper illustrate the potential of P-Y techniques to enhance both economic and environmental sustainability. For example, the laser inspection system in Case Study 2, while not directly preventing errors, ensures the removal of non-conforming products, thus preventing further processing and waste of resources. Similarly, the real-time

image detection system in Case Study 3, although not fully preventing mistakes, enables immediate error detection and correction, minimizing the production of defective products and associated waste.

## 8. Conclusions and future research

In conclusion, the Classification Graph serves as a valuable tool for companies seeking to improve their production processes through the effective implementation of P-Y techniques. By facilitating a rapid and objective evaluation of P-Y solutions, the Graph enables companies to identify areas for improvement, prioritize interventions, and optimize resource allocation. This, in turn, leads to cost savings, increased efficiency, and a positive impact on sustainability efforts.

Future research should focus on developing a comprehensive catalogue of P-Y techniques. This catalogue would assist companies in systematically designing effective P-Y solutions. Additionally, evaluations of proposed P-Y techniques should include a thorough analysis of their economic impact before implementation. This economic assessment should cover both the likelihood of mistakes reduction and the direct and indirect costs associated with the implementation of these techniques. Conducting such evaluations is essential to ensure that decisions regarding the adoption of specific P-Y solutions are economically justified and sustainable.

## References

- Amaral, L. C., Biazussi, J. L., Almeida, S. D., Gomes, F. J., & Araujo, D. A. (2023, October). Quick Response for Risk Mitigation in Oil Services Operations: A Case Study of Poka-Yoke Application. In *Offshore Technology Conference Brasil* (p. D032S055R003). OTC.
- Andersen M., Andersen R., Larsen C., Moeslund T. B. and Madsen O. (2009). Interactive Assembly Guide Using Augmented Reality. *Proceedings of the 5th International Symposium on Advances in Visual Computing (ISVC2009)*, Las Vegas, Nevada, 999-1008.
- Antonelli D., Stadnicka D. (2016). Classification and efficiency estimation of mistake proofing solutions by Fuzzy Inference. *IFAC Conference on Manufacturing Modelling, Management and Control*. June 28-30, 2016. Troyes, France. *IFAC-PapersOnLine*, 49(12):1134-1139. Web of Science.
- Antonelli, D., Stadnicka, D. (2019). Predicting and preventing mistakes in human-robot collaborative assembly. *IFAC-PapersOnLine*, 52(13): 743-748. <https://doi.org/10.1016/j.ifacol.2019.11.204>
- Azuma R., Baillet Y., Behringer R., Feiner S., Julier S. and MacIntyre B. (2012). Recent advances in augmented reality. *Computer Graphics and Applications IEEE*, 1(6):34-47.
- Chen L.H., Chang F. M. and Chen Y.L. (2011), The application of the multinomial control charts under inspection error. *International Journal of Industrial Engineering*, 18(5):244-253.
- Chimienti V., Iliano S., Dassisti M., Dini G. and Failli F. (2010). Guidelines for implementing augmented reality procedures in assisting assembly operations. *Proceedings of the 5th IFIP, Precision Assembly Technologies and Systems. IFIP Advances in Information and Communication Technology*, 315:174-179.
- Czajka P., Giesko T., Matecki K. and Zbrowski A. (2010). Methods and system of laser inspection of seal assembly in rolling bearings. *Technologia i Automatykacja Montażu*, 2:22-28 (in Polish).
- Dahari, S., Talib, M. A., & Gapor, A. A. (2025). Robust Control Chart Application in Semiconductor Manufacturing Process. *Journal of Advanced Research in Applied Sciences and Engineering Technology*, 43(2), 203-219.
- de Saint Maurice G., Giraud N., Ausset S., Auroy Y., Lenoir B. and Amalberti R. (2011). Comprendre la notion de détrompage. *Annales françaises d'anesthésie et de réanimation*, 30:51-56.
- Evans J. R. and Lindsay W. M. (2005). *The management and control of quality* (6th ed.). Thomson, South-Western, United Kingdom.
- Garza F. & Das M. (2001). On real time monitoring and control of resistance spot welds using dynamic resistance signatures. In *Circuits and Systems. MWSCAS 2001. Proceedings of the 44th IEEE 2001 Midwest Symposium*, 1:41-44.
- Gladysz, B., & Buczacki, A. (2018). Wireless technologies for lean manufacturing—a literature review. *Management and Production Engineering Review*, 9:20–34.
- Hakkarainen M., Woodward C. and Billingham M. (2008). Augmented Assembly using a Mobile Phone. *7th IEEE International Symposium on Mixed and Augmented Reality (ISMAR2008)*, 167–168.
- Hollnagel E. (2004). *Barrier analysis and accident prevention*. Ashgate.
- Kozikowski, E., Hartman, N. W., Camba, J. D. (2022). Development and evaluation of a computer vision system for assembly bolt pattern traceability and poka-yoke. *Proceedings of ASME 2022 17th International Manufacturing Science and Engineering Conference, MSEC 2022*, 2, art. no. V002T06A023.
- Kumar S., Kumar S.S.M. and Kumar A. (2009). Scrap reduction by using total quality management tools. *International Journal of Industrial Engineering*, 16(4):364-369.
- Lazarevic, M., Mandic, J., Sremcevic, N., Vukelic, D., & Debevec, M. (2019). A systematic literature review of Poka-Yoke and novel approach to theoretical aspects. *Strojnicki Vestnik/Journal of Mechanical Engineering*, 65(7-8), 454-467.
- Lucantoni, L., Antomarioni, S., Ciarapica, F. E., & Bevilacqua, M. (2022). Implementation of Industry 4.0 Techniques in Lean Production Technology: A Literature Review. *Management and Production Engineering Review*, 13:83-93.
- Mabkhot, M.M.; Ferreira, P.; Maffei, A.; Podrżaj, P.; Mądziel, M.; Antonelli, D.; Lanzetta, M.; Barata, J.; Boffa, E.; Finżgar, M.; Paško Ł.; Minetola P.; Chelli R.; Nikghadam-Hojjati S.; Wang V.; Priarone P.C.; Litwin P.; Stadnicka D.; Lohse N. (2021). Mapping Industry 4.0 Enabling Technologies into United Nations Sustainability Develop-

- ment Goals. *Sustainability* 2021, 13, 2560. <https://doi.org/10.3390/su13052560>
- Martinelli, M.; Lippi, M.; Gamberini, R.: Poka yoke meets deep learning: a proof of concept for an assembly line application. *Appl. Sci.* 12(21), 11071 (2022). <https://doi.org/10.3390/app122111071>
- Middleton P. (2001). Lean software development: two case studies. *Software Quality Journal*, 9:241-52.
- Muharam M. and Latif M. (2019), Design of poka-yoke system based on fuzzy neural network for rotary machinery monitoring, IOP Conference Series: Materials Science and Engineering, Volume 602, Conference on Innovation in Technology and Engineering Science (CITES 2018) 08/11/2018– 09/11/2018 Padang, West Sumatra, Indonesia.
- Pinosova, M., & Andrejiova, M. (2023). Analysis of the error rate in PCB production using quality management tool. *Annals of Faculty Engineering Hunedoara – International Journal of Engineering*. Tom XXI, 4:27-34.
- Rahardjo, B., Wang, F. K., Yeh, R. H., & Chen, Y. P. (2023). Lean manufacturing in industry 4.0: a smart and sustainable manufacturing system. *Machines*, 11(1), 72.
- Ramadan M. and Salah B. (2019), Smart Lean Manufacturing in the Context of Industry 4.0: A Case Study, *International Journal of Industrial and Manufacturing Engineering*, No. 3, Vol. 13, pp. 174–181.
- Saurin T. A., Ribeiro J. L. D., Vidor G. (2012). A framework for assessing poka-yoke devices. *Journal of Manufacturing Systems*, 31:358-366.
- Sellappan N., Palanikumar K. (2013). Modified prioritization methodology for risk priority number in failure mode and effects analysis. *International Journal of Applied Science and Technology*, 3(4):27-36.
- Shingo S. (1988). *Zero quality control: source inspection and the poka-yoke system*. Productivity Press.
- Stadnicka, D., and Antonelli, D. (2019). Human-robot collaborative work cell implementation through lean thinking. *International Journal of Computer Integrated Manufacturing*, 32(6): 580-595.
- Stewart M. and Grout R. (2001). The human side of mistake-proofing. *Production and Operations Management*, 10(4):440-459.
- Tkaczyk S. and Jagła J. (2001). The economic aspects of the implementation of a quality system process in Polish enterprises. *Journal of Materials Processing Technology*, 109:196-205.
- Trojanowska, J., Husár, J., Hrehova, S., & Knapčíková, L. (2023). Poka Yoke in Smart Production Systems with Pick-to-Light Implementation to Increase Efficiency. *Applied Sciences*, 13(21), 11715.
- Valles A., Noriega S., Sanchez J., Martínez E. and Salinas J. (2009). Six Sigma improvement project for automotive speakers in an assembly process. *International Journal of Industrial Engineering, Special Issue: Six Sigma – Its Application, Practice and Utility*, 16(3):182-190.
- Wyskiel M. (2014). Kaizen, as a form of continuous improvement in Lean culture – example of kitting line for assembly sets reorganization. IV Conference Lean Learning Academy "Lean Tools implementation in improvement projects". May 2014 Rzeszow, unpublished work (in Polish).
- Xiuxu Z. (2011) A Process Oriented Quality Control Approach Based on Dynamic SPC and FMEA. *International Journal of Industrial Engineering*, 18(8):244-253.
- Yin X., Fan X., Gu Y., and Wang J. (2017), Sequential dynamic gesture recognition controlled poka-yoke system for manual assembly, *CIMS*, No. 7, Vol. 23, pp. 1457–1468.
- Yoo S. H., Kim D. S. and Park M. S. (2012). Lot sizing and quality investment with quality cost analyses for imperfect production and inspection processes with commercial return. *Int. J. Production Economics*, 140:922-933.
- Yusuf, Y. B., & Halim, M. S. (2023). Stationary spot welding (ssw) quality improvement using six sigma methodology and a poka yoke jig design. *Journal of Engineering Science and Technology*, 18(1), 210-226.

## COMPACT VOC EMISSION TEST CHAMBER

### KOMPAKTOWA KOMORA DO BADAŃ EMISJI LOTNYCH ZWIĄZKÓW ORGANICZNYCH

Tomasz SAMBORSKI<sup>1,\*</sup>, Mariusz SICZEK<sup>1</sup>, Andrzej ZBROWSKI<sup>1</sup>,  
Łukasz ŁOŹYŃSKI<sup>1</sup>, Stanisław KOZIÓŁ<sup>1</sup>

<sup>1</sup> Łukasiewicz Research Network – Institute for Sustainable Technologies, Kazimierza Pułaskiego 6/10, 26-600 Radom, Poland

\* Corresponding author: [tomasz.samborski@itee.lukasiewicz.gov](mailto:tomasz.samborski@itee.lukasiewicz.gov)

#### Abstract

The publication presents the test method and construction of a compact VOC emission test chamber. Volatile organic compounds (VOCs) are mainly occur in paint and construction materials containing chemical resins, bitumen, binders, adhesives, etc., as well as residues of unreacted monomers. VOC emission testing is carried out on product samples in environmental chambers in accordance with PN-EN ISO 16000-9. The developed chamber, together with a proprietary control and test parameter acquisition system, allows testing at a stabilized temperature and humidity of air washing over the sample at a specified rate. Qualitative identification and quantitative testing of compounds present in the air inside chambers is carried out using a chromatograph, and the test results are compared with regulations on permissible chemical pollutants in the air of buildings and in atmospheric air. The developed chamber with horizontal sample loading is another version of VOC chambers, developed in response to market demands, offered and implemented in research laboratories by the Łukasiewicz Institute for Sustainable Technologies in Radom.

**Keywords:** test methodology, VOC, health protection, building materials, control

#### Streszczenie

Publikacja przedstawia metodę badań oraz budowę kompaktowej komory do badań emisji lotnych związków organicznych. Lotne związki organiczne (VOC) występują głównie w wyrobach malarskich oraz budowlanych zawierających żywice chemoutwardzalne, bitumy, lepiszcza, kleje itp., a także pozostałości nieprzereagowanych monomerów. Badanie emisji VOC odbywa się na próbkach wyrobów w klimatyzowanych komorach zgodnie z normą PN-EN ISO 16000-9. Opracowana komora wraz z autorskim systemem sterowania i akwizycji parametrów badań pozwala na prowadzenie badań w stabilizowanej temperaturze i wilgotności powietrza omywającego próbkę z określoną prędkością. Identyfikację jakościową i badanie ilościowe związków występujących w powietrzu komór przeprowadza się za pomocą chromatografu, a wyniki badań porównuje z przepisami dotyczącymi dopuszczalnych zanieczyszczeń chemicznych w powietrzu budynków i w powietrzu atmosferycznym. Opracowana komora z poziomym załadunkiem próbek jest kolejną wersją komór VOC, powstałą w odpowiedzi na oczekiwania rynku, oferowanych i wdrażanych w laboratoriach badawczych przez Ł-ITEE w Radomiu.

**Słowa kluczowe:** metodyka badań, VOC, ochrona zdrowia, materiały budowlane, sterowanie

## 1. Introduction

Volatile organic compounds (VOCs) are mainly found in painting products (Afshari et al., 2003). They can also be found in numerous other building products made of plastics, containing chemically cured resins,

bitumen (Boczkaj et al., 2014), binders, adhesives, etc. (Liu et al., 2012), as well as residues of unreacted monomers. VOC emission testing is carried out on product samples in environmental chambers in accordance with PN-EN ISO 16000-9, "Indoor air.



Part 9: Determination of the emission of volatile organic compounds from building products and furnishing. Emission test chamber method” (PN-EN ISO 16000-9). Thermostatic chambers at the appropriate temperature and humidity, and ventilated at a certain speed are used for testing (Koziol et al., 2019; Wei Wenjuan et al., 2012; Zhibini et al., 2003). Qualitative identification and quantitative testing of compounds present in the air inside chambers is carried out using a chromatograph (Demeestere et al., 2008; Niesłochowski, 2013; Ribes et al., 2007), and the test results are compared with regulations on permissible chemical pollutants in the air of buildings and in atmospheric air (Regulation of the Minister of Environment, 2002; Ordinance of the Ministry of Health and Social Welfare, 1996). VOC emission tests have become standard tests of hygienic properties of certain building products and materials, as well as common products (Oppl, 2014; Liu et al., 2012).

The rationale for carrying out the project is the need for an innovative solution (Invernizzi et al., 2021) that relies on the horizontal layout of the emission test chamber, which facilitates the placement of test objects inside it, especially those of higher mass. Another innovation is the ability to carry out tests at temperatures higher than those required by PN-EN ISO 16000-9, which makes it possible to accelerate tests and reproduce special conditions of use, such as intensively heated thermal roof insulation.

The results of the task are used in the design and manufacturing activities of the Institute's Prototyping Center, which for a number of years has been the developer and supplier of VOC emission test equipment kits to scientific (Fig. 1a) and industrial (Fig. 1b) laboratories in Poland (Koziol et al., 2019).



Fig. 1. Examples of VOV chambers implemented in: a) research centers, b) industry

## 2. The concept of the test chamber

The functional diagram of the VOC emission test stand (Fig. 2) was developed based on the recommendations in Annex C of PN-EN ISO 16000-9. In terms of functionality, three main modules can be distinguished: the emission test chamber, the air preparation module and the control system.

Emission test chambers and sampling system components in contact with emitted VOCs should be made of polished stainless steel or glass. The design of the chamber should provide:

- adequate tightness and strength to allow operation under positive pressure to avoid the

influence of the laboratory atmosphere on the measurement result,

- the ability to maintain temperature and humidity at the desired level,
- flow velocity of homogenized air over the surface of the test sample.

The purpose of the air preparation module is to supply the test space of the chamber with the appropriate amount of air of the desired purity and humidity.

The role of the control system is to maintain the set operating parameters of the test stand and to acquire and archive measurement data.

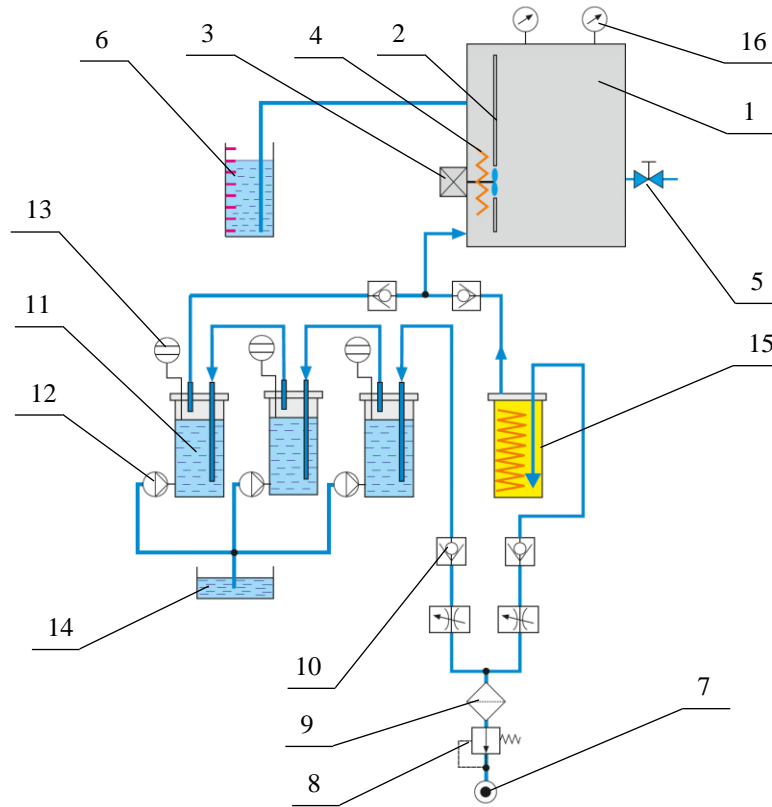


**Fig. 2.** Functional diagram of the test stand for testing VOC emissions: 1 - emission chamber, 2 - partition, 3 - fan, 4 - heater, 5 - sample intake valve, 6 - hydrostatic tank, 7 - compressor, 8 - pressure regulator, 9 - filter, 10 - check valve, 11 - washing bottle, 12 - pump, 13 - level gauge, 14 - buffer tank, 15 - dehumidifier, 16 - temperature and humidity sensor

**Table 1.** Basic parameters of the designed test chamber

Parameter	Value
Capacity	225 dm <sup>3</sup> ± 0.0045 dm <sup>3</sup>
Maximum operating pressure	500 Pa
Air temperature in the chamber	max +65°C
Relative humidity of the supplied air	max RH 50% ±5% RH
Air velocity at the sample surface	0.1 ÷ 0.3 m/s

### 3. Research device design

Based on the assumptions, virtual 3D CAD models of the complete device (Fig. 3) and all the elements that make up its structure were developed. The model was developed in Autodesk Inventor Professional.

Test chamber 1 is made of stainless steel and is the shape of a cuboid with a capacity of 225 liters (Fig. 4). It is equipped with a front door 2 with bolt locks 3. The required tightness of the test space is provided by a type 4 O-ring made of low-emission fluorocarbon-based rubber.

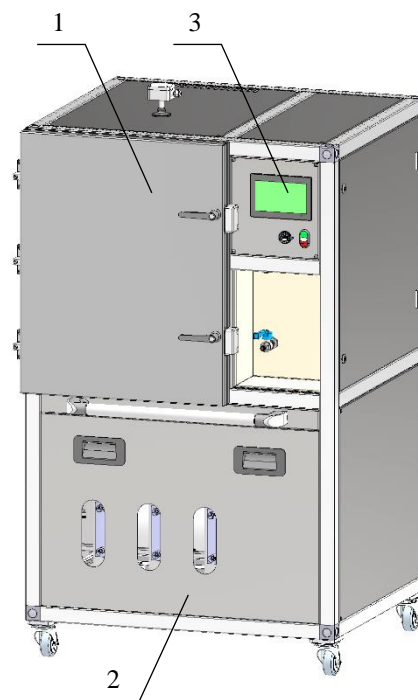


**Fig. 3.** CAD model of the VOC emissions testing device: 1 - test chamber, 2 - air preparation module, 3 - control system

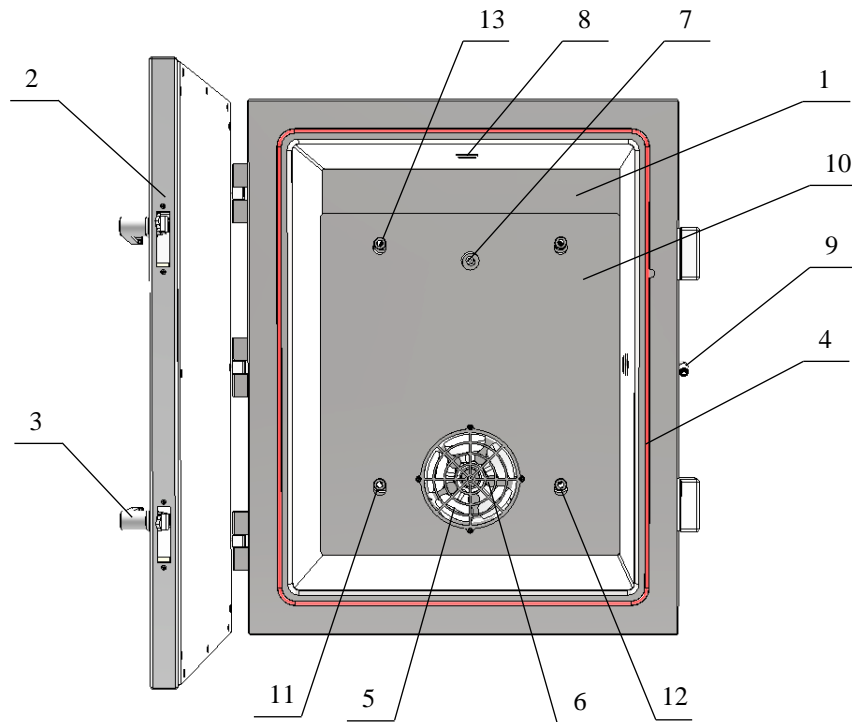


**Fig. 4.** CAD model of the test chamber: 1 - emission chamber, 2 - front door, 3 - bolt lock, 4 - seal, 5 - heating module, 6 - fan, 7 - temperature and humidity sensor, 8 - air velocity sensor grommet, 9 - air intake port, 10 - partition, 11 - dry air inlet, 12 - humid air inlet, 13 - air outlet

The proper circulation of air in the chamber, its homogenization and the flow of air at the appropriate speed around the samples is provided by a fan (6) with a drive located outside the chamber together with a partition (10). Heating module (5) is responsible for maintaining the set temperature during testing or warming up at the set temperature, such as 60°C. A temperature and humidity sensor (7) is located in the rear wall of the chamber. At the top of the chamber there is a grommet (8) that allows the insertion of an air velocity sensor washing over the tested sample. On the right side of the chamber, there is a port (9) connected to a ball valve for drawing the air to be analyzed. Symmetrically, on both sides of the fan are placed air inlets for dry (11) and humid (12) air. The flow of air through the chamber is provided by two fittings (13) located at the top of the chamber and connected to a water tank that provides positive pressure in the test chamber.

The air preparation module is located at the bottom of the test device (Fig. 5). The supporting structure is a rack (1) attached to two ball guides (2) that allow the

module to be pulled out from inside the unit for service purposes. An oil-free compressor (3) with a minimum output of 500 l/h is located at the rear of the rack. Compressed air flows through pressure regulator (4) and carbon filter (5). Pre-cleaned air is directed to two flow regulators (6). The first regulates the value of the air flow through three washing bottles connected in series, filled with demineralized water. The second regulates the value of the air flow through the dehumidifier (7) filled with silica gel. The ratio of the values of the humid and dry air streams is responsible for the humidity of the air supplied to the emission chamber, while the sum of the streams determines the air flow rate through the chamber.

Each washing bottle, which cleans and humidifies air, is equipped with an optical level gauge (8) and a water level sensor (13). The water level in the washing bottles is topped up automatically with peristaltic pumps (9) drawing water from a buffer tank (12). The dehumidifier is equipped with a sight glass that allows to visually assess the moisture level in the silica gel and decide whether it needs to be dried.



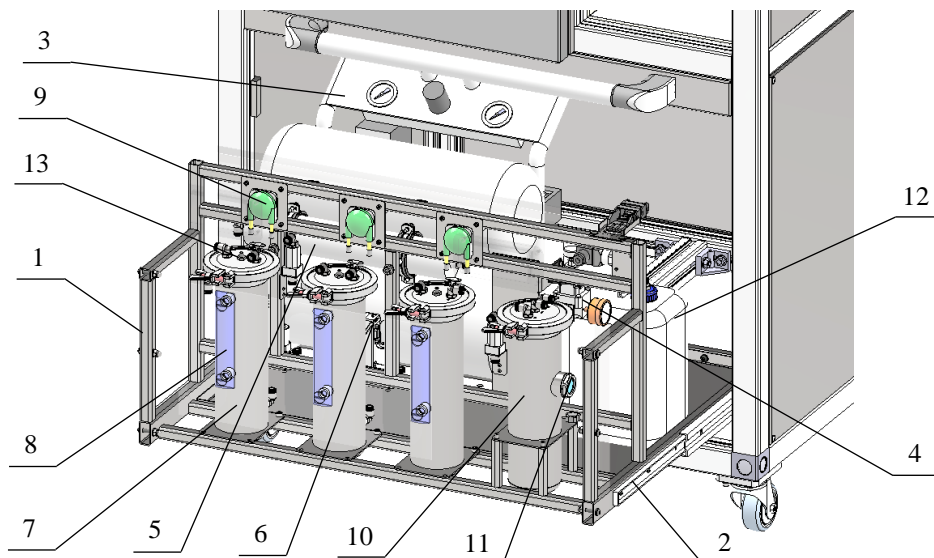


**Fig. 5.** Air preparation module: 1 - rack, 2 - ball guides, 3 - compressor, 4 - pressure regulator, 5 - carbon filter, 6 - air flow regulators, 7 - washing bottle, 8 - level gauge, 9 - peristaltic pump, 10 - dehumidifier, 11 - sight glass, 12 - buffer tank, 13 - level sensor

Modern equipment, and especially research equipment, is characterized by the integration of mechanical systems with advanced control systems. The designed control system (Fig. 6) provides the following functions:

- controlling the temperature of the air in the chamber,
- controlling the humidity of the air in the chamber,
- adjusting the amount of airflow through the chamber,
- adjusting the air velocity over the sample
- automatic replenishment of demineralized water level.

Regardless of the parameter settings, the control system will enable:

- writing a data record to the device memory every  $\frac{1}{2}$  h or 1 h,
- erasing device memory,
- browsing stored data records using the control panel,
- adjusting time and date displayed on the device (the set date and time are used to save the data record),
- adjusting the contrast of the control panel, operation in Polish and English.

The developed user interface will include graphical visualizations of the test processes carried out by the device. The use of mnemonic icons for the control panel interface (Fig. 7) is envisioned to facilitate menu navigation and simplify operation.

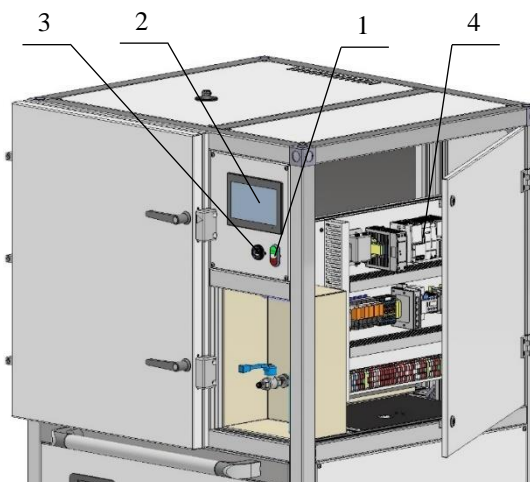


**Fig. 6.** VOC emission test chamber control system components: 1 - START-STOP button, 2 - control panel, 3 - RJ communication connection, 4 - PLC controller

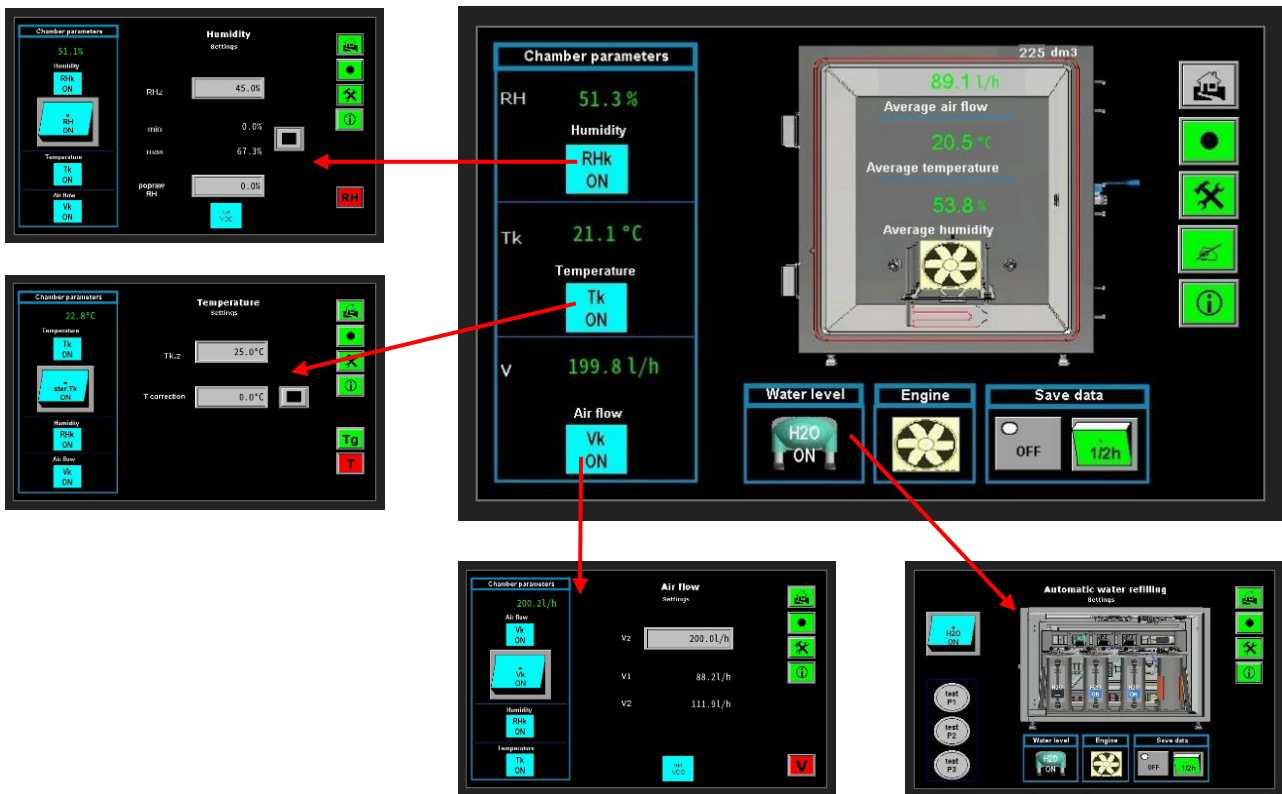


Fig. 7. Control panel screen design

### 4. Prototype verification

On the basis of the assumptions made and the model and technical documentation developed, a prototype VOC emission test stand with a horizontal emission chamber was built (Fig. 8).

The sampling port for air contaminated by the VOC emitted by the tested product (Fig. 9), is located in a recess in which a tank of water is placed to establish the positive air pressure in the chamber during testing.

In the process of verifying the prototype, test and operational studies were conducted under operating conditions consistent with the real ones.

The following inspection procedures were implemented to check the compliance of the device's operating parameters with normative requirements: checking cleanliness, tightness, airflow, temperature and humidity.



Fig. 8. Prototype of the test stand: 1 - emission chamber, 2 - control panel, 3 - air sampling port and water tank, 4 - pull-out shelf, 5 - air preparation module

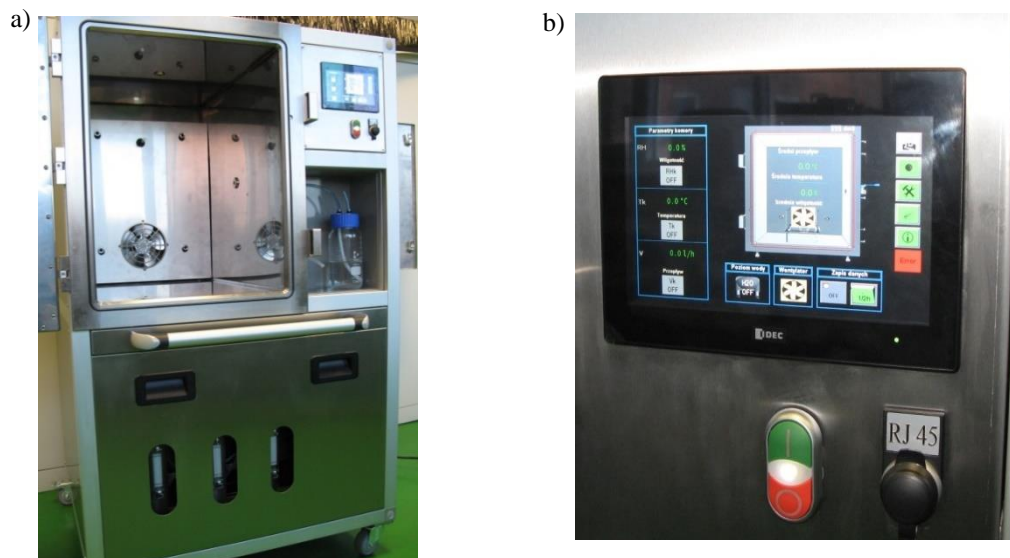


Fig. 9. Prototype of the test stand: a) view with the emission chamber open, b) control panel

#### 4.1. Checking cleanliness of the air in the emission chamber

In accordance with the standard PN-EN ISO 16000-9: Part 9, Section 8.2, the quality of the supply air should meet the following criteria:

- the concentration of total volatile organic compounds (TVOCs) in the chamber should be less than  $20 \mu\text{g}/\text{m}^3$ ,
- The concentration of a single targeted VOC in the chamber should be less than  $2 \mu\text{g}/\text{m}^3$ .

Air samples for testing were taken in accordance with ISO 16000-6:2021 ( $3 \text{ dm}^3$ , flow rate of  $6 \text{ dm}^3/\text{h}$ ). For adsorption of organic compounds, steel sorption tubes filled with 200 mg of Perkin Elmer Tenax TA were used and conditioned at  $300^\circ\text{C}$  before each analysis.

Determination of the concentration of VOCs was performed in accordance with PN-EN ISO 16017-

1:2006. A Perkin Elmer Clarus 680 gas chromatograph equipped with a Clarus 680C MS mass detector and TurboMatrix 650 ATD thermal desorber was used for the analysis. Certified reference material – VOC-Mix 12 from Restek was used for quantitative analysis. Concentrations of other organic compounds were obtained using the equivalent method for toluene. The list of identified compounds is shown in Table 2.

The chromatogram obtained by analyzing the air sample from the test chamber and by analyzing the standard solution is shown in Fig. 10.

The resulting sum VOC concentration does not exceed the concentration of the maximum allowable concentration of volatile organic compounds according to ISO 16000-6 “Determination of volatile organic compounds in indoor and test chamber air by active sampling on Tenax TA sorbent, thermal desorption and gas chromatography using MS or MS-FID”.

Table 2. List of identified compounds

Identified compound	Concentration on tube [ $\mu\text{g}$ ]	Actual concentration [ $\mu\text{g}/\text{m}^3$ ]
1,2-dichlorobenzene	0.004589	1.481
Cis-3,3,5-trimethylcyclohexanol	0.000210	0.068
Benzyl alcohol	0.000358	0.115
Butoxyethoxy ethanol	0.000126	0.041
3,3,5-trimethylcyclohexyl methacrylate	0.000112	0.036
<b>TOTAL VOC [<math>\mu\text{g}/\text{m}^3</math>]</b>		<b>1.741</b>

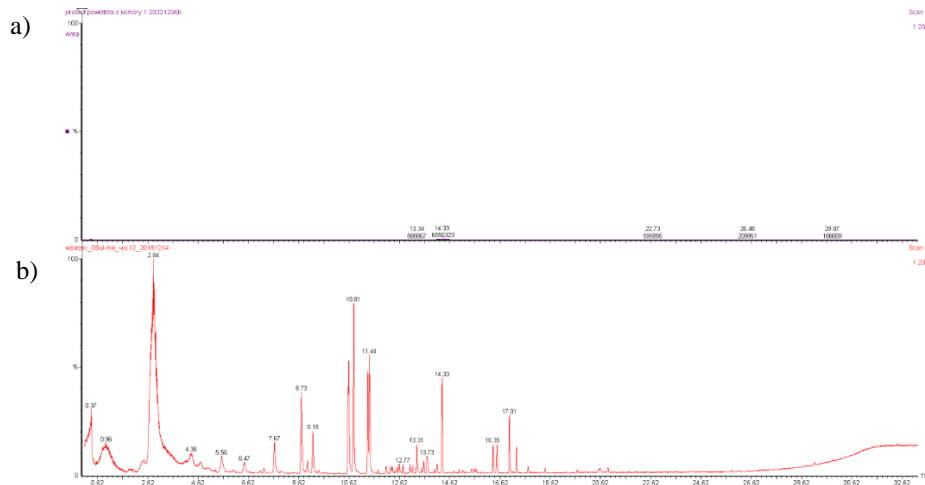


Fig. 10. Chromatogram obtained from the analysis of: a) air sample from the test chamber, b) standard solution

### 4.2. Tightness and airflow measurement

In accordance with EN ISO 16000-9: Part 9, Section 6.4 emission test chamber is considered air tight if the air loss is less than 5% of the air inlet flow. Two rotameters were used for testing. The first was connected between the output of the air preparation module supplying air to the chamber and its input. The other was connected to an open air sampling valve from the emission test chamber. A summary of the results of the airflow measurements is shown in Table 3.

Table 3. Airflow measurement results.

No.	Flow [dm <sup>3</sup> /h]			Loss [dm <sup>3</sup> /h]	Allowable loss [dm <sup>3</sup> /h]
	Set stream	Inlet stream	Outlet stream		
1	50 ±1	50 ±1	49 ±1	1	2.5
2	100 ±1	98 ±1	95 ±1	3	5
3	150 ±1	148 ±1	143 ±1	5	7.5
4	200 ±1	198 ±1	190 ±1	8	10
5	250 ±1	248 ±1	238 ±1	10	12.5

### 4.3. Temperature and humidity measurements

In accordance with EN ISO 16000-9: Part 9, Section 8.1 products intended for use in Europe should be tested at 23 °C ± 2 °C and RH 50% ± 5% during emission testing (ISO 554). The results of comparative measurements made with the chamber's instrumentation (thermo-hygrometer) and a reference gauge are shown in Tables 4 and 5.

Table 4. Temperature measurement results.

No.	Temperature [°C]			Absolute error [°C]	Allowable error [°C]
	set	thermo-hygrometer reading	reference gauge reading		
1	23	23.3 ±0.5	23.3 ±0.2	0.0	±2
2	24	24.0 ±0.5	24.04 ±0.2	0.04	±2
3	25	25.2 ±0.5	25.3 ±0.2	0.1	±2
4	50	52.4 ±0.5	50.5 ±0.2	1.9	±2

Table 5. Relative humidity measurement results.

No.	Humidity [%RH]			Absolute error [%RH]	Allowable error [%RH]
	set	thermo-hygrometer reading	reference gauge reading		
1	20	21.1 ±2	21.6 ±1	0.5	±5
2	40	40.4 ±2	41.7 ±1	1.3	±5
3	45	46.3 ±2	48 ±1	1.7	±5
4	50	50.7 ±2	53.1 ±1	2.4	±5

The results of the tests confirmed the readiness of the completed prototype to carry out standard tests of VOC emissions from samples of building materials, wood-based materials and other products emitting VOCs hazardous to health. Verification of the control system was also carried out towards the realization of the established test procedures. The tests confirmed the correct operation of the measurement and control system.

## 5. Conclusions

At the Łukasiewicz Institute for Sustainable Technologies in Radom, a prototype compact VOC emission test chamber has been developed and created, and has undergone comprehensive verification tests. The functional tests carried out confirmed the possibility of appropriate adjustment of the physical parameters of the implementation of emission tests while maintaining the air quality of purity required by the normative provisions for testing VOC emissions using the emission test chamber method. The design solution developed in the course of the work in the form of a horizontal VOC emission test chamber was used to fulfill an order for the supply of two test kits (Fig. 11) for a company producing wood-based insulation materials for the construction industry.



**Fig. 11.** View of implemented VOC emission test chambers

The original design solutions developed at Łukasiewicz - ITEE have been protected by industrial design registration (Rp.xxxxx).

## References

Afshari A., Lundgren B., Ekberg L. E. (2003). Comparison of three small chamber test methods for the measurement of VOC emission rates from paint. *Indoor air*, 13, 156-165.

- Boczka G., Przyjazny A., Kamiński M. (2014). Characteristics of volatile organic compounds emission profiles from hot road bitumens. *Chemosphere*, 107, 23-30.
- Demeestere K., Dewulf J., De Roo K., De Wispelaere P., Van Langenhove H. (2008). Quality control in quantification of volatile organic compounds analysed by thermal desorption-gas chromatography-mass spectrometry. *Journal of Chromatography*, 1186, 348-357.
- Invernizzi M., et al. (2021). Lights and shadows of the VOC emission quantification. *Chemical Engineering Transactions*, 85, 109-114.
- Kozioł S., Matecki K., Samborski T., Siczek M., Wojutyński J., Zbrowski A. (2019). Overpressure chamber for testing in high air purity conditions. *Journal of Machine Construction and Maintenance*, 114, 81-90.
- Liu WeiWei, et al. (2012). Indoor decorating and refurbishing materials and furniture volatile organic compounds emission labeling systems: A review. *Chinese Science Bulletin*, 57, 2533-2543.
- Niesłochowski A. (2013). Badanie emisji lotnych związków organicznych (VOC) techniką termicznej desorpcji i chromatografii GC-MS. *Prace Instytutu Techniki Budowlanej*. Vol. 42, 9-20.
- Oppl R. (2014). New European VOC emissions testing method CEN/TS 16516 and CE marking of construction products. *Gefahrstoffe-Reinhaltung der Luft*, 74, 62-68.
- PN-EN ISO 16000-9:2009 Indoor air. Determination of the emission of volatile organic compounds from building products and furnishing. Emission test chamber method.
- Ribes A, Carrera G., Gallego E., Roca X., Berenguer M.A., Guardino X. (2007). Development and validation of a method for air-quality and nuisance odors monitoring of volatile organic compounds using multi-sorbent adsorption and gas chromatography/mass spectrometry thermal desorption system. *Journal of Chromatography A*, 1140, 44-55.
- Regulation of the Minister of Environment dated 5 December 2002 on reference values for certain substances in the atmosphere (Journal of Laws of 2003, No. 1, item 12),
- Wei Wenjuan, et al. (2012). A standard reference for chamber testing of material VOC emissions: design principle and performance. *Atmospheric Environment*, 47, 381-388.
- Ordinance of the Ministry of Health and Social Welfare dated 12 March 1996 on the permissible concentrations and intensities of harmful factors for health, emitted by building materials, equipment and elements of equipment in rooms intended for human occupation (Official Journal of the Republic of Poland of 1996, No. 19, item 231).
- Zhibini Z. et al. (2003). Determination of Volatile Organic Compounds in Residential Building. Proceedings of the International Conference on Indoor Air Quality Problems and Engineering Solutions, <https://doi.org/10.1177/1420326X9600500404>.

## CONCEPT OF AUTOMATED CAR BATTERY ASSEMBLY LINE

### KONCEPCJA ZAUTOMATYZOWANEJ LINII MONTAŹU BATERII SAMOCHODOWYCH

Jacek DOMIŃCZUK<sup>1</sup> , Małgorzata GAŁAT<sup>2</sup>

<sup>1</sup> Department of Information Technology and Robotics in Production, Lublin University of Technology, Nadbystrzycka 36 street, Lublin, Poland

<sup>2</sup> CER, Energetyków 17 street, Lublin, Poland

\* Corresponding author: j.dominczuk@pollub.pl

#### Abstract

This paper presents the concept of an automotive battery assembly line. The line includes in its structure fully and semi-automated assembly sockets, as well as manual assembly sockets. The transport between the sockets is carried out using an AGV autonomous trolley system. The selection of the assembly process execution method was based on an analysis of the technical feasibility of the process as well as an analysis of the occupation time of individual assembly stations. The resulting line structure indicates to what extent the automation of the assembly process contributes to a change in material flow and influences the way the process is carried out, including a variety of technical means used. The paper presents an analysis of the use of particular workstations. As a criterion for optimization, the occupation time was taken in relation to the cycle time, which translates into the optimal use of resources involved in the production process.

**Keywords:** automation, transport, assembly

#### Streszczenie

W artykule przedstawiono koncepcję linii montaŹu baterii samochodowych. Linia ta zawiera w swojej strukturze gniazda montaŹowe w pełni zautomatyzowane, częściowo zautomatyzowane oraz gniazda montaŹu ręcznego. Transport pomiędzy gniazdami realizowany jest z wykorzystaniem systemu wózków autonomicznych AGV. Wybór sposobu realizacji procesu montaŹu został oparty na analizie możliwości technicznych realizacji procesu jak również analizie czasu zajęcia poszczególnych stanowisk montaŹowych. Otrzymana struktura linii wskazuje w jakim stopniu automatyzacja procesu montaŹu przyczynia się do zmiany przepływu materiałów i wpływa na sposób realizacji procesu, w tym na różnorodność zastosowanych środków technicznych. W pracy zaprezentowano analizę wykorzystania poszczególnych stanowisk roboczych. Analiza ta posłuŹyła do przeprowadzenia optymalizacji przebiegu linii montaŹu komponentów. Jako kryterium optymalizacji przyjęto czas zajęcia stanowiska w stosunku do czasu cyklu co przekłada się na optymalne wykorzystanie zasobów zaangażowanych w proces produkcyjny.

**Słowa kluczowe:** automatyzacja, transport, montaŹ

## 1. Introduction

Every manufacturing company aims to achieve maximum production efficiency at the lowest possible cost (Więcek-Janka, Pawlicki i Walkowski, 2018). In an era of constant market volatility, technology development and strong competition, the product manufacturing process requires continuous improve-

ment. Each improvement can affect the success or failure of a company. This means that the production process should be constantly analysed in order to eliminate imperfections and increase production efficiency and quality (Stadnicka, Lean manufacturing, 2021). It is therefore important for the proper functioning of a production enterprise to



optimally design individual operations, i.e. production activities, into an appropriate sequence. Improper planning of the sequence of operations leads to unnecessary costs and increased production time. Attempts to sequence manufacturing processes have been made for a long time and are reflected in many methods e.g. Gantt charts, network planning methods, etc. (Brzozowska & Gola, 2021).

The issue of streamlining production preparation processes appears to be very important as companies strive for ever shorter production cycles. The streamlining of processes is forced not only by the desire to reduce production costs, but above all by the need to operate competitively in the market. The use of modern tools in all phases of product design, preparation and production is helpful in creating such conditions (Stadnicka, Problemy w obszarach produkcyjnych, 2021).

The end of the production preparation cycle is organisational preparation. The type of production depends on the degree of specialisation and workload of individual workstations (Gola, 2021). We can categorise basic types of production as mass production, batch production and unit production. Depending on the type of production, workstations are classified as:

- universal - operations and parts are not strictly assigned; universal equipment and tools,
- specialised - having a specific group of parts and operations assigned, together with the possibility of limited changeovers,
- special - strict allocation of parts and operations without the possibility of changeovers.

The manufacture of parts and their assembly are components of the production process. In the manufacturing process, a semi-finished product undergoes changes in shape, dimensions and other functional characteristics, and is then transformed into a finished part. In the assembly process, parts are joined together to form sub-assemblies or directly into a finished product. Fig. 1. shows the relationship between the manufacturing and assembly processes against the background of the production process. Assembly, in the sense of product and material flow, is related to the manufacturing process, while in the sense of information flow it is integrated with production control, process and production planning, product development and indirectly with marketing and product planning (Koch, 2006).



Fig. 1. Assembly as an element of the production process (Koch, 2006)

The main determinants for the selection of an appropriate assembly method at the assembly system design stage are, on one hand, the products to be assembled, the process and production characteristics, and, on the other hand, economic criteria such as manufacturing costs, the number of production shifts,

etc. Based on these principles, assembly methods can be divided into six types (Koch, 2006):

- manual assembly,
- manual assembly with technical tool support,
- mechanical assembly with universal devices,

- mechanical assembly using specialised equipment,
- automatic assembly using programmable feeding systems (Domińczuk i Gałat, 2023),
- automatic assembly using industrial robots.

The analysis of a product requires the characteristics of the parts that it is composed of and the features of the connections between these parts. These characteristics affect the complexity of the assembly process and the required execution time. The design rules are based on two characteristics: shortening the number of assembly operations and simplifying them. Reducing the number of operations can be achieved, among other things, by designing modular construction of products and eliminating an excessive number of components, according to the criterion of the purpose of their presence. Assembly operations can be simplified as a result of the analysis of design rules, e.g. the main direction of assembly, the system of feeding, manipulating and consociating of objects, or good accessibility to individual components (Rudawska i inni, 2023).

A robotic assembly system is defined as a structure consisting of personnel, one or more assembly robots and flexible peripheral equipment for assembling individual objects or components into a finished product. The personnel perform functions to support and supervise assembly work, e.g. related to system implementation, pallet stock replenishment, supervision, programming and system management. Assembly robots perform operations connected with manipulation of objects in the system (Kaczmarek i Panasiuk, 2018). The peripheral equipment is responsible for the automation of the feeding of parts to the assembly, the use of appropriate tools, sensors, control systems, as well as safety (Łapczyńska, 2023).

Robotic assembly systems are built in two basic configurations (Koch, 2006):

- robotic assembly sockets; they require the use of independent units consisting of one or more robots and peripheral equipment to carry out the assembly of a product; the characteristics of this structure are a relatively long work cycle and a large number of different objects assembled by a single robot,
- robotic assembly lines; this system combines several workstations installed in a line; the characteristics of this structure are a short work cycle, a limited number of assembly of different objects by each robot and the need to transport the product between different workstations; a robotic line may also consist of several sockets, connected by a transport system, with the possibility of using buffers between them.

The choice of the degree of mechanisation and automation is primarily related to the production programme. It is obvious that it is totally different to design a technological process for a few pieces of a product and quite different for a large series or mass production. The degree of mechanisation and automation is also influenced by the requirement for quality and repeatability of the product. It is known that in order to achieve high quality and repeatability of the product, special machines or devices will most often be needed, and it will be necessary to follow certain principles of repetitive basing and fixing of individual elements of the often complex product.

The purpose of this study is to present the possibility of assembling automotive batteries using automated workstations. The achieved efficiency of these workstations means that they can be used repeatedly during the assembly process at different stages. The result is a reduction in the amount of technical means used, which reduces production costs. The paper presents the concept of a technical solution that allows the use of technical means used in battery assembly in such a way as to minimize production costs. The presented solution is designed to increase production efficiency by combining automated stations with manually operated stations in a single assembly line. The proposed solution was developed for an actual car battery. Due to commercial confidentiality, the details of the battery assembly process are not provided in the study.

## 2. Design requirements

A car battery is to undergo the assembly process (Jones, 2024). A general structure of an electric car battery is shown in Fig. 2. This is an illustrative scheme. The battery consists of a number of components that need to be assembled together to form a finished product (Warner, 2015). The assembly process involves various assembly methods appropriate for the task being performed.

Fig. 3. shows a block diagram of the assembly of the battery components. It takes into account the assembly of both the elements constituting the battery enclosure, a cooling system, power modules, control and power management elements and additional battery equipment. It was assumed that transport between sockets would be carried out using an AGV autonomous trolley system. Due to the quality requirements of the process, the execution of some assembly operations must be carried out automatically. This applies, for example, to the thermal compound application operation. The requirement here is to maintain a constant cross-section of the applied bend of the compound. This operation can only be



carried out using a robotic workstation additionally equipped with a process control system (Fig. 4.). This requires that the battery assembly time does not exceed 226 seconds. As can be seen from the presented diagram of operations included in the assembly process, both fully-automated, semi-automated and

manual assembly workstations should be used to complete the task. The use of manual assembly is mainly related to the need to execute the assembly of flexible cables, which are not adapted to the automatic assembly process.

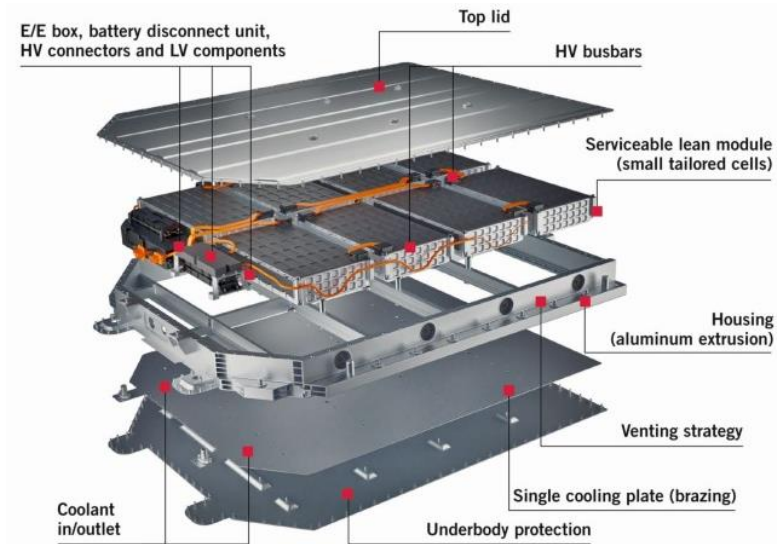


Fig. 2. Components of the electric car battery (Rudolph, Teuber, Beykirch i Löbberding, 2023)

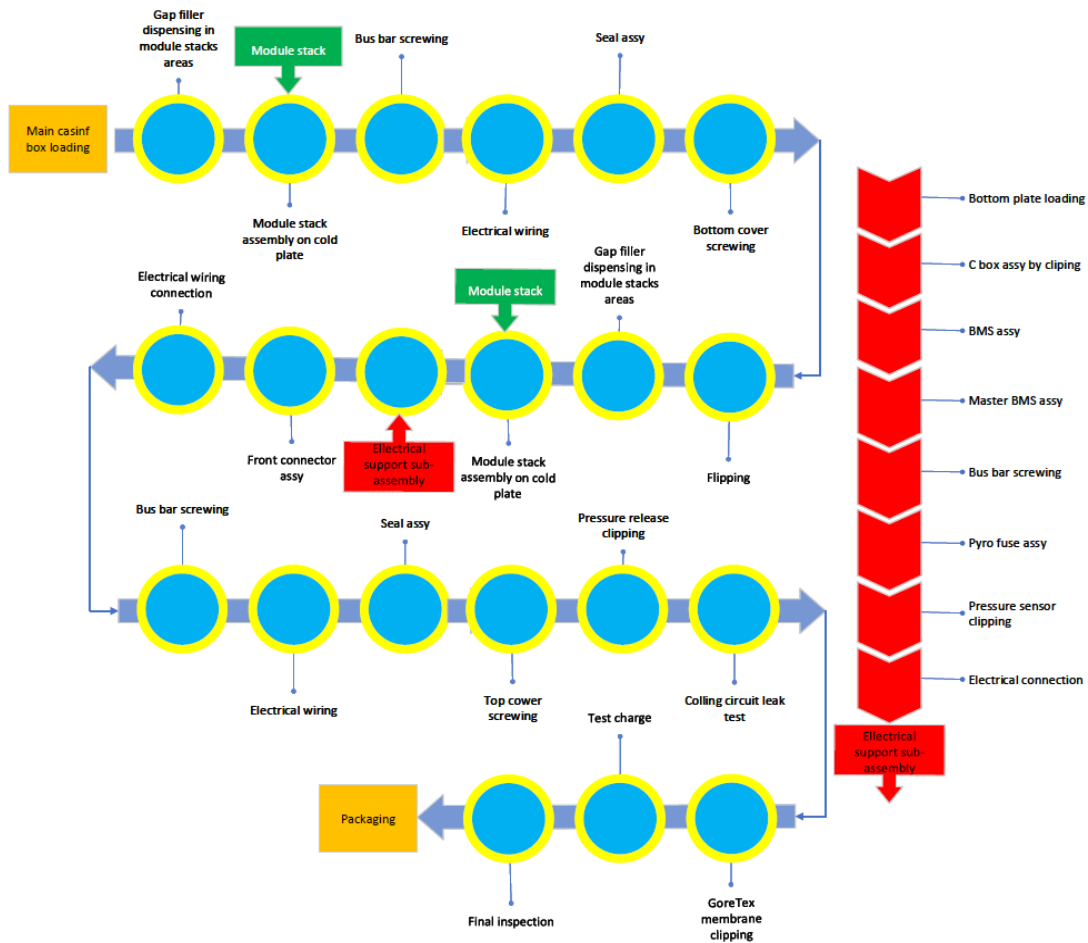


Fig. 3. Diagram of battery assembly

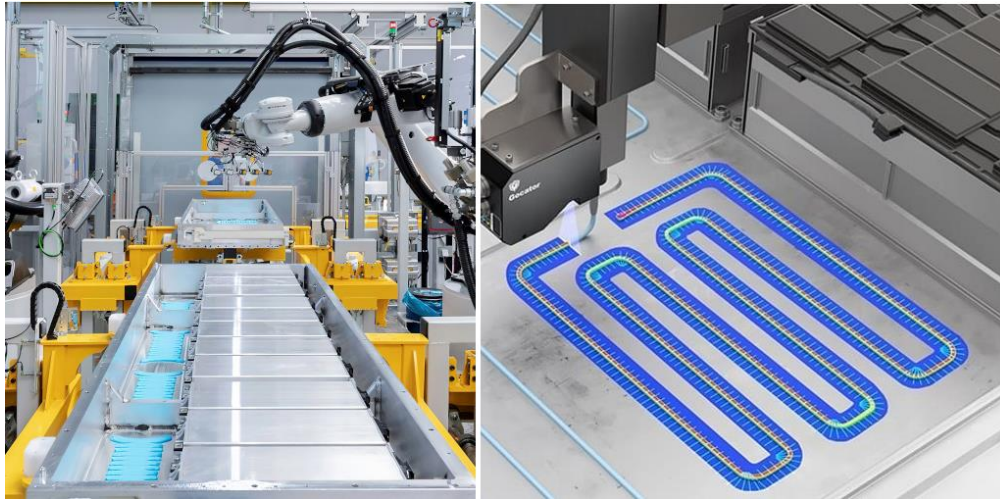


Fig. 4. Process of application of thermal compound (E-mobility engineering, 2024)

In order to optimise the course of the assembly process, a time analysis of the individual tasks was carried out (Fig. 5.). This analysis made it possible to

define the course of the assembly process, taking into account the optimum use of the assumed technical resources.

STATION 1 - Loading components				STATION 7 - Lift, Rotation				STATION 13 TOP floor assembly			
Operation	Time/Qt	Qt	TIME [s]	Operation	Time/Qt	Qt	TIME [s]	Operation	Time/Qt	Qt	TIME [s]
Unloading&Loading Bottom	90	1	90.0 M	Modules lift	16	1	16.0 A	Busbar assembly	20	3	60 M
Transfer component AMR	26	1	26 A	Rotation + transfer	28	1	28.0 A	front connector assy	60	1	60.0 M
<b>Total time</b>			<b>116</b>	MODULES Assembly	20	1	20.0 A	Transfer component	26	1	26 A
				Transfer component	40	1	40 A	<b>Total time</b>			<b>146</b>
				<b>Total time</b>			<b>104</b>				
STATION 2 - Robot Filler gap dispensing				STATION 8 - Screwing				STATION 14 - Manual operations - 2 operators (13 +14)			
Operation	Time/Qt	Qt	TIME [s]	Operation	Time/Qt	Qt	TIME [s]	Operation	Time/Qt	Qt	TIME [s]
Filler gap dispensing Bottom	0.04	2179.3	87.2 A	Screwing (ground, std)	7	20	140.0 A	loading cover on station fireman access assy	10	1	10.0
Transfer component	26	1	26 A	Robot park position + work position	8	1	8.0 A	fireman access stocking inside and outside	45	1	45.0
Filler gap dispensing Top	0.04	2179.3	87.2 A	Transfer component ROTATION	16	1	16 A	Loading TOP seal assembly	25	1	25.0
Transfer component	26	1	26 A	<b>Total time</b>			<b>164</b>	loading top cover	20	1	20.0
<b>Total time</b>			<b>226</b>					cooling circuit leak test ATEQ	160	1	160.0
								loading 4x clip on conveyor	15	4	60.0
								Transfer component	26	1	26
								<b>Total time</b>			<b>212</b>
STATION 3 - Robot module assembly				STATION 9 - Rotation BATTERY				STATION 15			
Operation	Time/Qt	Qt	TIME	Operation	Time/Qt	Qt	TIME [s]	Operation	Time/Qt	Qt	TIME [s]
Module assembly Bottom	20	4	80.0 A	Modules lift	16	1	16.0 A	Robot work position	4	1	4.0
Transfer component	26	1	26 A	Rotation + transfer	28	1	28.0 A	Screwing (ground, std)	7	22	154.0
Module assembly TOP	20	4	80.0 A	Unloading on AMR	16	1	16.0 A	Robot park position	4	1	4.0
Transfer component	26	1	26 A	Transfer component	30	1	30 A	pressure release clipping (x2) BIG	15	2	30.0
<b>Total time</b>			<b>212</b>	<b>Total time</b>			<b>90</b>	Transfer component	32	1	32
								<b>Total time</b>			<b>224</b>
STATION 4 - Robot screwing				STATION 10 - ELECTRIC BOARD PREPARATION				STATION 16			
Operation	Time/Qt	Qt	TIME [s]	Operation	Time/Qt	Qt	TIME [s]	Operation	Time/Qt	Qt	TIME [s]
Module screwing x4 Bottom	14	4	56.0 A	bottom plate loading on station	8	1	8.0 M	pack leak test ATEQ	160	1	160.0
Transfer component	26	1	26 A	master bms assy - screwing	8	4	32.0 M	Gore membrane assy x 2	15	2	30.0
Module screwing x4 TOP	14	4	56.0 A	BMS slave assy (x8)	8	8	64.0 M	Transfer component	32	1	32
Transfer component	26	1	26 A	P-sensor & Pyrofuse assembly	8	2	16.0 M	<b>Total time</b>			<b>222</b>
<b>Total time</b>			<b>164</b>	C-Box fixation	10	4	40.0 M				
				Transfer component	16	1	16 A				
				<b>Total time</b>			<b>176</b>				
STATION 5 - TRANSFER				STATION 11 TOP floor assembly				STATION 17			
Operation	Time/Qt	Qt	TIME [s]	Operation	Time/Qt	Qt	TIME [s]	Operation	Time/Qt	Qt	TIME [s]
Pick up top cover with modules and put on bottom cover with modules				TOP to BOTTOM busbar screwing	20	2	40.0 M	CONNECTION	8	3	24.0 M
Towers fixation	10	2	20 M	Main harness assembly	16	1	16.0 M	EOL tests & chargefinal	1200	1	1200.0 A
Harnesses assembly	10	4	40 M	Electric board assembly	10	3	30.0 M	Transfer component	40	1	40 A
Bus bar screwing Bottom	20	3	60 M	36v connector fixation	10	5	50.0 M	<b>Total time</b>			<b>211</b>
Transfer component	40	1	40 A	RCS800 connector assembly	10	6	60.0 M				
<b>Total time</b>			<b>160</b>	Transfer component	26	1	26 A				
				<b>Total time</b>			<b>196</b>				
STATION 6 - Loading components (TOP)				STATION 12 TOP Floor assembly				STATION 18			
Operation	Time/Qt	Qt	TIME [s]	Operation	Time/Qt	Qt	TIME [s]	Operation	Time/Qt	Qt	TIME [s]
Unloading&Loading TOP	90	1	90.0 M	APEX280 connector assembly	10	4	40 M	final inspection and labelling	10	3	30.0 M
Loading seal on bottom	26	1	26 M	BMS to Modules harness assembly	10	12	120.0 M	Unloading&Loading BATTERY	90	1	90.0 M
Transfer component ROTATION	16	1	16 A	Busbar assembly	20	2	40 M	Transfer component	32	1	32 A
<b>Total time</b>			<b>132</b>	Transfer component	26	1	26 A	<b>Total time</b>			<b>152</b>
				<b>Total time</b>			<b>226</b>				

Fig. 5. Analysis of occupation time of assembly sockets (in [s])

### 3. Assembly line design

The analysis of the possibility of executing the battery assembly, taking into account the optimum time of use of technical means, made it possible to develop a diagram of the assembly line (Fig. 6.). In the solution, it was assumed that the base component for the first stage of assembly will be placed on an AGV trolley on a stand with manual operation (Fig. 7.). At

stands 2, 3 and 4, the assembly process will be fully automatic and will involve all the steps connected with assembling the battery modules on both the bottom and top sides of the battery (Fig. 8.). Stations 5 and 6 are manually operated due to the execution of operations that are difficult to automate. Stations 7, 8 and 9 are fully automated and the concept of their operation is based on cooperation with station 6

resulting in a partially automated socket (Fig. 9.). At the subsequent stations up to station 14, the assembly process is carried out manually. Stations 15 and 16 (Fig. 10.) are automated. Stations 17 and 18 (Fig. 11.) are manually operated with the assumption that the

work at these stations will be carried out by operators from the preceding stations. This is done to minimise interruptions in or er to make optimal use of resources.

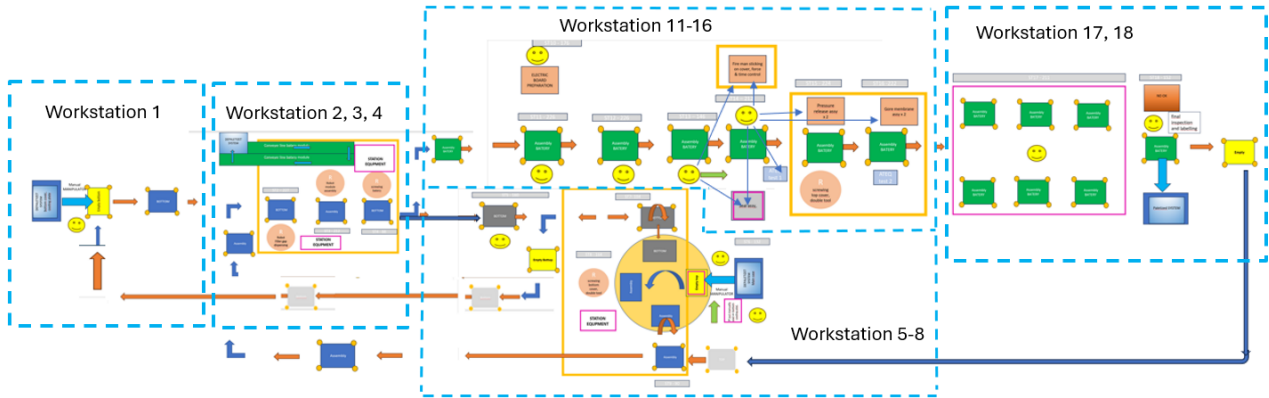


Fig. 6. Diagram of assembly line

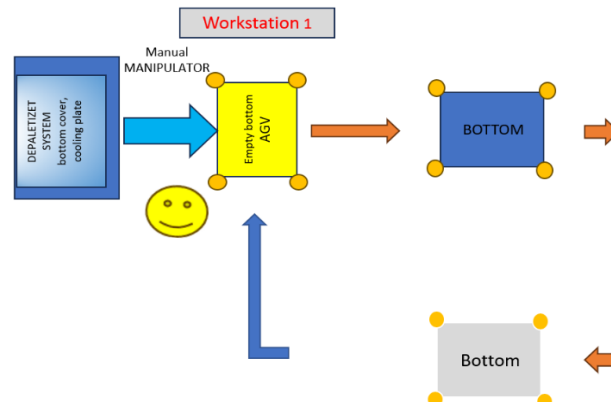


Fig. 7. Diagram of workstation 1

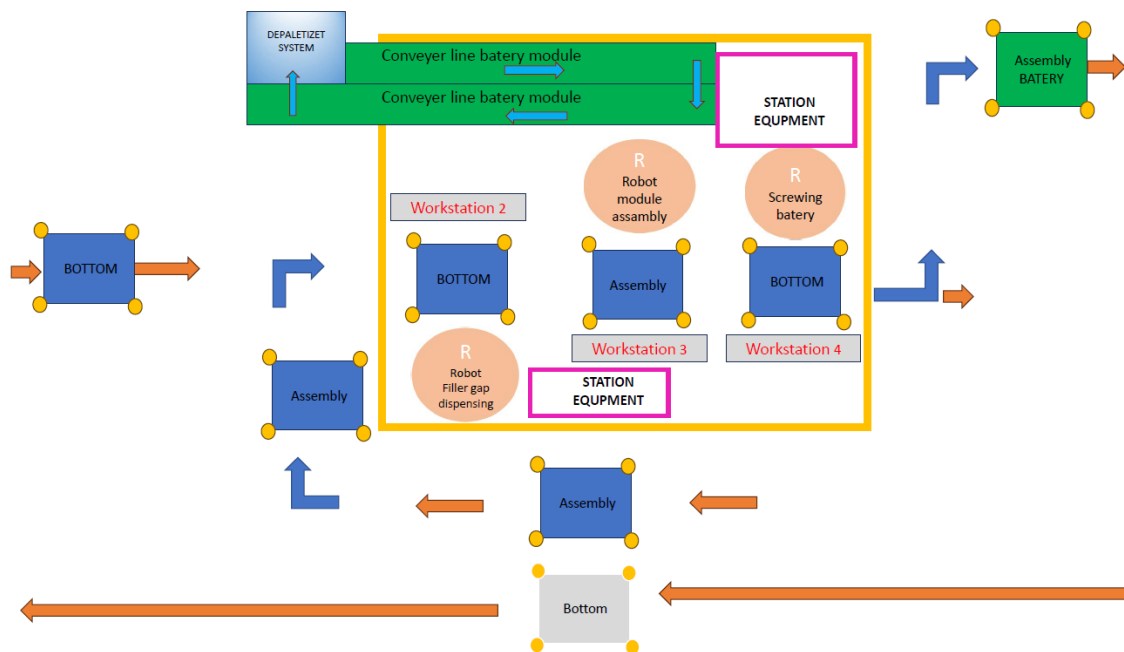


Fig. 8. Diagram of workstations 2, 3, 4

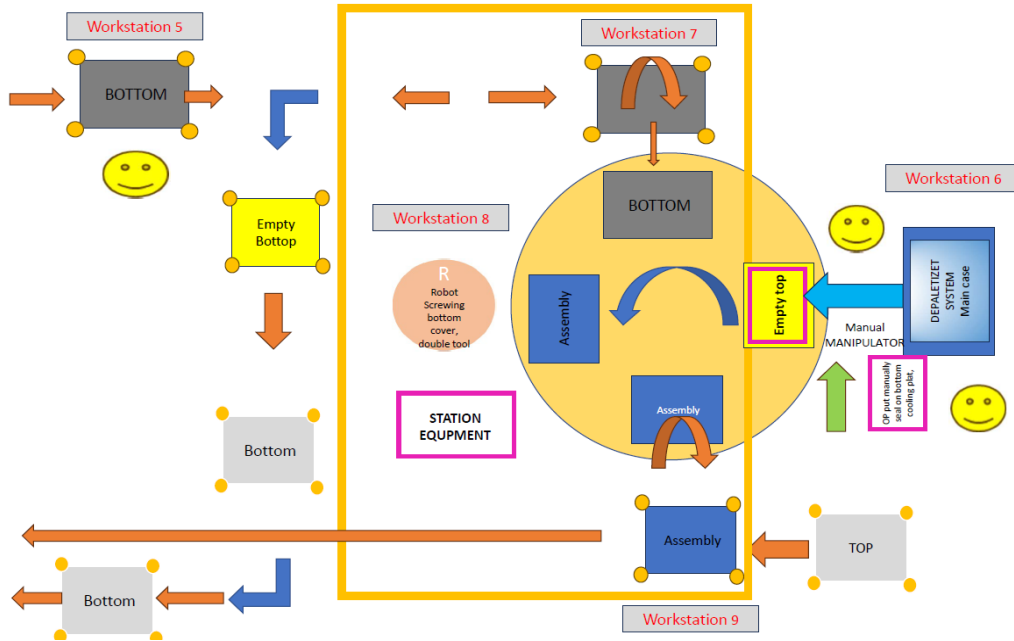


Fig. 9. Diagram of workstations 5-9

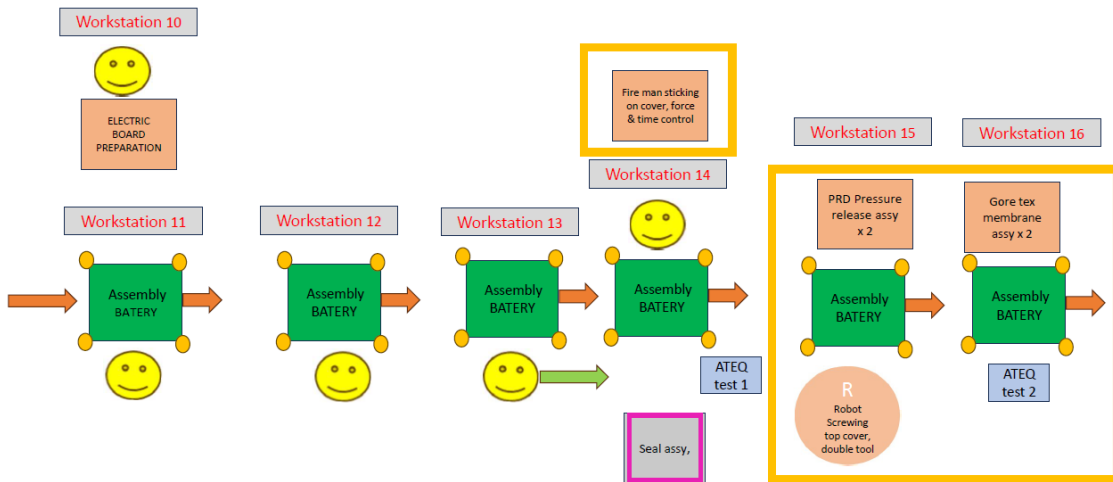


Fig. 10. Diagram of workstations 10-16

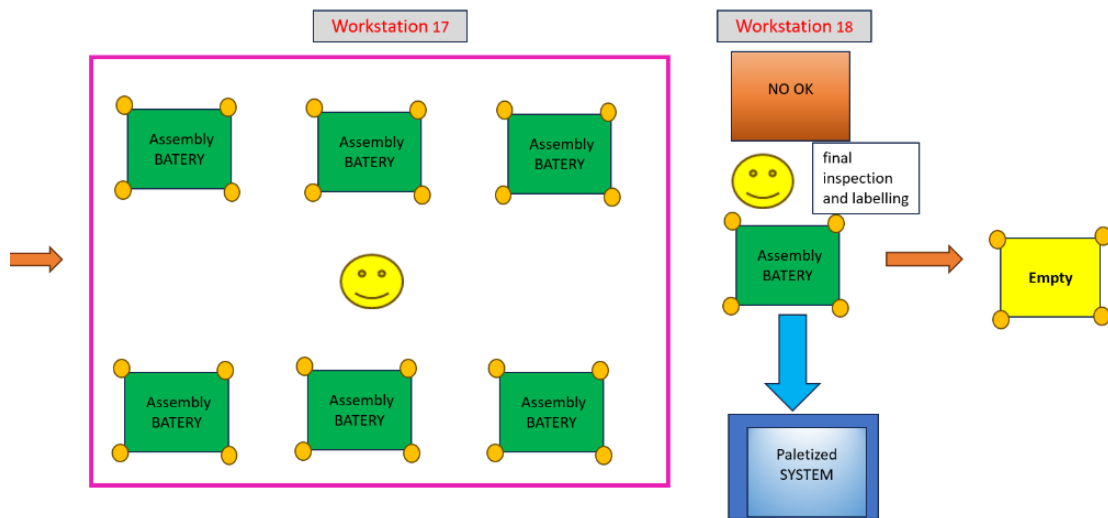


Fig. 11. Diagram of workstations 17, 18

Equal distribution of tasks between positions allows to maintain a constant work tact. At the same time, it should be noted that positions in which manual labor predominates should have additional time. This time is needed to compensate for differences in employee productivity.

#### 4. Summary

The solution for the electric car battery assembly line presented in this paper allows to obtain optimal conditions for the process to be achieved while minimising the technical resources involved. Works that are difficult and costly to automate were left to be performed in a manual system. Those that are susceptible to automation and at the same time important in terms of the quality of the assembly process are to be carried out in automated assembly sockets. Due to the high cost of automation, the product flow was planned so as to make maximum use of the possibilities of the technical solutions used, including robots. Attention was paid to the need to use a minimum of transport means as well as tooling for moving the product along the assembly line. Thanks to the division of operations used, it was possible to separate two transport lines with independent means of transport. This division makes it much easier to manage the mobile robots and also to respond to abnormal situations.

The presented solution is an innovative solution aimed at minimising the cost of implementing a new product in the assembly process. This solution meets the expectations of Industry 4.0 (Stadnicka, et al., 2022) (Kolberg & Zuhlke, 2015) (Brzowska & Gola, 2021). The presented solution is the result of searching for optimal conditions of process execution, which is one of the basic activities during the design of robotic production systems (Cha, Vogel-Heuser i Fischer, 2020).

The presented assembly system is based on a modular design, which makes it easily adaptable to other industrial applications. It can be scaled and adapted to new application needs. All these factors make the system concept versatile and universally applicable for a wide range of required performance variants including full automation.

The presented solution combines two assembly methods: automatic and manual. The increase in the degree of automation changes the way products flow. Due to the higher efficiency of the automated process, there is an opportunity to use robotic stations to perform repetitive activities. This results in the possibility of directing products to repetitive activities on the line. Thanks to such an assembly run, automated stations are optimally loaded in terms of their working

time. In order to implement such a run, the use of AGVs is recommended. The use of mobile robots makes the presented concept a flexible solution. It can be adapted to specific applications by merely changing the product flow path. The occupation time of the workstation was adopted here as an evaluation criterion, aimed at minimizing the interruption time in the overall assembly time of 226 s. This approach provides an opportunity to reduce the amount of technical resources involved in the production process. When configuring the layout, special attention was paid to minimizing the number of workers required to operate the line. They carried out tasks that are difficult to complete in an automated process. All repetitive activities were carried out at automated stations.

The presented solution can be used during the development of car battery assembly lines. Increasing the degree of automation of the assembly process will be possible after eliminating from the battery design elements that are not susceptible to automatic assembly. This will make the assembly process more efficient. It is therefore expedient to look for design solutions for increasing the degree of automation of the process.



#### References

- Brzowska, J., & Gola, A. (2021). Computer aided assembly planning using MS Excel software – a case study. *Applied Computer Science*(17(2)), pp. 70-89. doi:<https://doi.org/10.35784/acs-2021-14>.
- Cha, S., Vogel-Heuser, B., & Fischer, J. (2020). *Analysis of metamodels for model-based production automation system engineering*. The Institution of Engineering and Technology. doi:<https://doi.org/10.1049/iet-cim.2020.0013>.
- Domńczuk, J., & Gałat, M. (2023). Automated system of inter-operational transport with a pneumatic drive. *Assembly Techniques and Technologies*, pp. 13-19. doi:<https://doi.org/10.7862/tiam.2023.4.2>.
- E-mobility engineering*. (2024, 04 04). Retrieved from <https://www.emobility-engineering.com/automated-battery-manufacturing/>.
- Gola, A. (2021). *Biblioteka Cyfrowa Politechniki Lubelskiej*. Retrieved from <https://bc.pollub.pl/dlibra/publication/14005/edition/13663>.
- Jones, N. (2024). *The electric-car battery revolution*. Londyn: Nature Publishing Group. doi:10.1038/d41586-024-00325-z.
- Kaczmarek, W., & Panasiuk, J. (2018). *Robotyzacja procesów produkcyjnych*. Warszawa: PWN.
- Koch, T. (2006). *Systemy zrobotyzowanego montażu*. Wrocław: Oficyna Wydawnicza Politechniki Wrocławskiej.
- Kolberg, D., & Zuhlke, D. (2015). Lean Automation enabled by Industry 4.0 Technologies. *IFAC-PapersOnLine*(3), pp. 1870-1875. doi:<https://doi.org/10.1016/j.ifacol.2015.06.359>.

- Łapczyńska, D. (2023). The possibilities of improving the human-machine co-operation in semi-automatic production process. *Assembly Techniques and Technologies*, pp. 30-36. doi:<https://doi.org/10.7862/tiam.2023.1.4>.
- Rudawska, A., Domińczuk, J., Miturska-Barańska, I., Doluk, E., Szabelski, J., & Gola, A. (2023). *Podstawy technologii montażu*. Wydawnictwo Politechniki Lubelskiej.
- Rudolph, M., Teuber, M., Beykirch, R., & Löbberding, H. (2023, 01 30). Technology Trends in High-voltage Battery Development. *Springer Nature*. doi:<https://doi.org/10.1007/s38313-023-1484-x>.
- Stadnicka, D. (Ed.). (2021). *Lean manufacturing*. Rzeszów: Oficyna Wydawnicza Politechniki Rzeszowskiej.
- Stadnicka, D. (Ed.). (2021). *Problemy w obszarach produkcyjnych*. Rzeszów: Oficyna Wydawnicza Politechniki Rzeszowskiej.
- Stadnicka, D., Sęp, J., Amadio, R., Mazzei, D., Tyrovolas, M., Stylios, C., . . . Navarro, J. (2022). Industrial Needs in the Fields of Artificial Intelligence, Internet of Things and Edge Computing. *Sensors*. doi:<https://doi.org/10.3390/s22134501>.
- Warner, J. (2015). *The Handbook of Lithium-Ion Battery Pack Design*. Elsevier. doi:<https://doi.org/10.1016/C2013-0-23144-5>.
- Więcek-Janka, E., Pawlicki, J., & Walkowski, P. (2018). Przykład wprowadzania usprawnień w procesach produkcyjnych. *Zeszyty Naukowe Politechniki Poznańskiej*, 271-282. doi:10.21008/j.0239-9415.2018.076.20.

## USING DRONES AND ARTIFICIAL INTELLIGENCE TO ASSESS DAMAGE IN AIRCRAFT ASSEMBLY JOINTS

### UŻYCIE DRONÓW ORAZ SZTUCZNEJ INTELIGENCJI W PROCESIE OCENY USZKODZEŃ POŁĄCZEŃ MONTAŹOWYCH SAMOLOTU

Marcin KRYSIAK<sup>1,\*</sup> , Filip KUBIK<sup>1</sup> 

<sup>1</sup> The Faculty of Mechanical Engineering and Aeronautics, Rzeszów University of Technology, Powstańców Warszawy 12, 35-959 Rzeszów, Poland

\* Corresponding author: 163614@stud.prz.edu.pl

#### Abstract

Rapid development of Artificial Intelligence (AI) technologies in recent years has created new opportunities to address the growing challenges in the aviation industry. Machine learning and Deep Learning, particularly through Convolutional Neural Networks (CNNs), have advanced image recognition capabilities, enhancing inspection processes possibilities. This paper explores the integration of AI with drones to improve the precision, efficiency, and speed of inspections of airframe emphasizing the necessity of accurate equipment preparation and precise operational planning. The study demonstrates how AI algorithms can process high-resolution images and sensor data to identify and classify defects. The motivation for this paper is to address the critical need for more efficient inspection methods in aviation, driven by the industry's increasing demand for higher repair process throughput and stringent safety standards.

**Keywords:** artificial intelligence, image recognition, drones, defects detection

#### Streszczenie

Szybki rozwój technologii sztucznej inteligencji (SI) w ostatnich latach stworzył nowe możliwości radzenia sobie z rosnącymi wyzwaniami w przemyśle lotniczym. Metody uczenia maszynowego i głębokiego uczenia, szczególnie za pomocą konwolucyjnych sieci neuronowych (CNN), poprawiły zdolności rozpoznawania obrazów, usprawniając możliwości procesów inspekcji. Niniejszy artykuł opisuje propozycję integracji SI z dronami i w celu poprawy precyzji, efektywności i szybkości inspekcji płatowców podkreślając konieczność dokładnego przygotowania sprzętu i precyzyjnego planowania operacji. Tekst omawia przetwarzanie obrazów wysokiej rozdzielczości i danych z czujników, identyfikując i klasyfikując uszkodzenia. Motywacją do omówienia danego tematu jest konieczność opracowania bardziej efektywnych metod inspekcji w lotnictwie, co wynika z rosnącego zapotrzebowania na większą przepustowość procesów napraw i rygorystyczne standardy bezpieczeństwa w branży.

**Słowa kluczowe:** sztuczna inteligencja, rozpoznawanie obrazów, drony, wykrywanie uszkodzeń

## 1. Introduction

In recent years, there has been observed a tremendous development in technologies related to Artificial Intelligence. This revolution has not bypassed aviation sector, which has been facing

numerous industry challenges, such as decreasing availability of raw materials and tightening legal requirements. The aircraft manufacturing, assembly and inspection industry is extremely complex within the meaning of its smooth and accuracy operation level requirements. Therefore, there is the demand for



significant involvement of modern solutions that facilitate and speed up the work.

The need to accelerate and improve maintenance processes in aviation can be observed by looking at current forecasts related to aircrafts production volume, which clearly indicate the necessity to increase the capacity of service units (Zachariah, Sharma, Kumar, 2023). Currently, problems arising in aviation companies also require quick and reliable solutions. Recent issues with geared turbofan (GTF) engines produced by Pratt & Whitney have significantly impacted the operations of many airlines. As a result, European carrier WizzAir had to ground over 40 aircraft (Garbuno, 2024). Following a shocking incident during a Boeing 737 Max 9 flight, where evacuation doors were torn off shortly after take-off, investigation discovered anomalies in how they were attached to the fuselage (National Transport Safety Board, 2024).

Artificial Intelligence has an untapped potential to execute and speed up maintenance processes by using algorithms and machine learning techniques enabling workers to complement traditional quality control methods and increase the precision and efficiency of supervision operations. AI-based systems can analyse vast amounts of data in real-time, enabling proactive identification of potential defects and anomalies during the process. This approach not only reduces the risk of errors, but also ensures that aircraft meet rigorous safety standards.

Moreover, combining data analysis with algorithms and delivering images from cameras mounted on drones or virtual reality (VR) goggles could result in significantly facilitating maintenance processes in service organisations, thereby leading to increase of the industry's development pace.

The next part of the paper presents the goal of the work and the applied methodology. The third section describes the capabilities and limitations of AI systems focusing on data processing. The following chapter covers image recognition technologies development considering latest technological advancements. Subsequently, the paper discusses types of data collected and industry sectors actively utilising drones while the sixth section of the work shows current solutions based on image recognition algorithms in aviation manufacturing. The final chapters describe the proposed concept of a System Assessing Damage in Aircraft Assembly Joints and provide the summary of AI usage in process of assessing structural damages.

Based on current literature, the proposed system allows for combining capabilities of these technologies in the aviation industry, leading to further

enhancement of the efficiency and accuracy of processes in the aircraft production and inspection. The work focuses on applications in detecting cracks in the airframe structure as well as damaged rivets.

## 2. Goal and work methodology

Rapidly advancing technology significantly facilitates the accomplishment of complex AI systems into existing solutions. Market needs and trends in aviation clearly indicate the necessity of a new solution development that support maintenance processes.

The aim of this work is to propose the integrated system that could meet those needs. To achieve this goal, literature review is conducted regarding Artificial Intelligence, its construction and abilities in data processing (Step 1). Then the focus changes to Image Recognition where possibilities regarding current technologies and AI implementation in this field are discussed (Step 2). Additionally, drones' employment for the real time image collection is analysed (Step 3), as well as current AI technologies used in aviation are reviewed (Step 4). This is to expand and combine existing solutions into a system with new capabilities (Step 5).

The work methodology is summarized in the Table 1 containing each step, method conducted, and output received.

**Table 1.** Methodology and received output

	Step	Method	Output
1	Exploration of AI capabilities	Literature Review	Data processing capabilities
2	Research of Image Recognition technologies	Literature Review	Deep learning models
3	Analysis of drones' deployment	Review of current applications	Technological possibilities
4	Review of AI technologies in aviation	Research of existing solutions	Current AI implementations
5	Development of a new concept	Analyzing needs and capabilities	A new concept of a System Assessing Damage in Aircraft Assembly Joints

After examining the limitations and possibilities of existing solutions, an integrated multifunctional system is proposed, combining various technologies to facilitate daily work in construction inspection. The work includes a conceptual description of how such system operates, highlighting the use of existing systems and the associated limitations.



### 3. Artificial Intelligence – Capabilities and limitations

Artificial Intelligence (AI) offers a wide range of possibilities that significantly impact society, economy and transformation of many fields. One of the most promising aspects of AI is its ability to automate routine tasks by machine learning techniques utilisation and automatization. AI may take over many repetitive jobs, such as quality control in manufacturing, data management or customer service (Kuittinen, 2024). This results in increased efficiency, cost reduction and may free employees' time up for more creative and strategic work.

Artificial Intelligence enables quick and effective analysis of vast amounts of data, which can be used in the identification of significant patterns, trends and relationships (Milson, Bruce, 2024). One significant limitation is its dependence on the quality and quantity of presented data. Poor data quality or insufficient data can lead to inaccurate and biased outcomes. Additionally, AI systems often require substantial computational power and resources, which can be costly. Another limitation is the lack of contextual understanding, which means processing information and making predictions based only on known patterns without any of the nuanced perception humans have. Furthermore, ethical concerns arise among the society (e.g. data privacy), security and the potential perpetuation or even exacerbation existing biases. Therefore, cautious approach, ensuring reliable ethical standards and addressing limitations, is necessary in the development and implementation processes, despite comprehensive potential of Artificial Intelligence (Kaushikkumar, 2024).

### 4. Image recognition

Image recognition is one of the oldest areas of Artificial Intelligence development, which beginning is dated back to the 1950s and has grown to today's advanced technologies. In 1950, British computer scientist Alan Turing proposed the concept of a "learning machine", which initiated research into Artificial Intelligence (Copeland, Proudfoot, 2007). The first attempts at image recognition were made in the 1960s, focusing on simple tasks such as identifying handwritten characters using rule-based methods and simple shape analysis (Andreopoulos, Tsotsos, 2013). At the end of the 20th century, Yann LeCun and his team introduced Convolutional Neural Networks (CNN) through the LeNet model, which succeeded in recognizing handwritten digits (LeCun et al., 1998). The increase in computing power and the availability of larger datasets enabled the development of more advanced algorithms. A breakthrough appeared in

2006 when Geoffrey Hinton and his team introduced Deep Neural Networks, making deep learning possible to be achieved (Hinton, Osindero and Teh, 2006). This resulted in revolutionary achievements in competitions like ImageNet, where Neural Networks began to show the potential of deep learning in image recognition tasks (Deng et al., 2009).

Image recognition is an intelligent technique for identifying and detecting objects or features in a digital image. The process assigns labels to objects extracted from a scene, which means that image recognition assumes that objects in the scene have been extracted as individual elements. Extraction of characteristic features is possible for Artificial Intelligence by using various visual techniques such as edge detection, image segmentation and feature extraction (Javidi, 2002). Edge detection allows algorithms to identify the boundaries of object, while image segmentation divides it into more understandable parts. Feature extraction involves identifying significant characteristics of objects which help in their identification process. Typical image recognition algorithms are used in operations such as optical character recognition, pattern matching, face recognition, license plate matching, scene identification, and detecting changes in scenes (Javidi, 2002).

Machine Learning and Deep Learning methods are useful approaches to image recognition (Bagheri, Akbari and Mirbagheri, 2019). In the Machine Learning approach, key features of the image, which are identified and extracted, are used as inputs to the model. On the other hand, Deep Learning focuses on models based on the structure and function of the brain, known as Neural Networks. The most commonly used models are Convolutional Neural Networks (Long, Shelhamer and Darrell, 2015). These are used to learn significant patterns from image samples and identify those features in newly processed images.

Despite significant progress in the field of image recognition, there are certain challenges that limit and complicate the operation of such models. Image recognition often requires taking context into account and dealing with dynamically changing conditions, for example distinguishing between a cat sitting on a table and a cat sitting on the floor can be difficult for such systems. Artificial Intelligence may struggle to recognize images under variable conditions, such as changing lighting, perspective or weather. This phenomenon can occur particularly in video surveillance structure or autonomous systems, where conditions are unpredictable (Javidi, 2002). Furthermore, the effectiveness of Machine Learning algorithms mostly depends on the quality and diversity of the training data set. An absence of data variety can lead to

overfitting or underfitting of models, which affects ability to properly recognize images (Javidi, 2002). However, continuous development and advances in sensory technologies (high-resolution cameras, 3D scanners) are facilitating collecting increasingly detailed image data.

## 5. Employing drones for data acquisition

Drones are capable of gathering a variety of data types such as aerial imagery, videography, thermal imaging, multispectral and hyperspectral imaging, photogrammetry, environmental sensor data and geophysical sensor data. Aerial imagery and videography are based on capturing high-resolution photos and videos, which are used in mapping, surveying, and monitoring processes (Pargieła, 2023). Moreover, images can be captured by using thermal imaging which detects heat differences. This solution is making invaluable support for applications like search and rescue operations or inspecting infrastructure looking for heat loss or other issues. Multispectral and hyperspectral imaging capture data across various wavelengths, which is particularly useful for agricultural analysis, environmental monitoring, and detecting specific material properties (Yao, Qin and Chen, 2019).

Furthermore, drones play a significant role in agriculture supporting controlling process. Unmanned Aerial Vehicle (UAV) can enhance effectiveness of crop monitoring, identifying pest infestations and managing irrigation. Drones are used in the construction and infrastructure sectors for site surveying, conducting topographic maps and monitoring construction work progress (Nex, Remondino, 2014). They are also crucial for inspecting infrastructure such as bridges, buildings, power lines, which enhance maintenance and safety by providing detailed and current information (Yao, Qin and Chen, 2019).

Another field where drones have made a remarkable impact is environmental monitoring. They are used in wildlife conservation to track animal movements, monitor habitats and assess biodiversity. In forestry, drones support management of forest health, monitoring illegal logging activities and conducting fire appraisal (Sun et al., 2023). Disaster management efforts also benefit from UAV technology by involving drones in search and rescue missions to locate missing people and assess deterioration in disaster-stricken areas (Zwęgliński, 2020).

The advantages of using drones for data acquisition are considered because UAV missions are cost-effective, reducing the need for expensive manned aircraft or extensive ground surveys. They enhance safety by allowing data collection in

hazardous or inaccessible areas without risking human beings. Providing high-end sensors can result in precision, delivering superior images and accurate measurements. Furthermore, various sensors can be carried to collect different types of data depending on the specific needs of a project.

## 6. The utilization of image recognition technologies and Artificial Intelligence in aviation

Current literature positions indicate the usage of image recognition in the process of identifying aircraft airframe damage, including various types of structural element joints. The work (Brandoli et al., 2021) discusses the application of Artificial Intelligence to detect corrosion on aircraft fuselages. The authors present a methodology for utilizing Machine Learning algorithms to analyse image and sensor data, providing the automatic identification of corroded areas. Portable Data Acquisition and Integration System (DAIS) for non-destructive testing is used to capture images of the airframe. Solution contains charge-coupled device (CCD) camera and a double pass retroreflection projected onto the screen. The study employs advanced image processing techniques, Neural Networks, and classification models, which have been tested on real data collected during aircraft inspections. The results show that the application of AI significantly improves the accuracy and efficiency of corrosion detection compared to traditional inspection methods.

Another notable paper (Amosov, Amosova and Iochkov, 2022) explores usage of Deep Neural Networks for recognizing defects in rivet joints during the manufacturing processes of aircraft parts. The authors describe a methodology for employing advanced Artificial Intelligence algorithms to analyse and recognize images of rivet joints, enabling the automatic and accurate detection of defects. The image is captured by a manipulator arm moving along a pre-planned path according to the design documentation. The manipulator arm is equipped with video cameras positioned at various angles, laser rangefinders, and Light Emitting Diode (LED) lights. The accuracy of defect detection is influenced by several external factors: lighting direction, flickering, reflections, shadows, and image angle. The LEDs create directional lighting to mitigate external influences on the examined surface. The obtained data undergoes preliminary information processing and a detection and classification system, after which the final information is transmitted to the operator's monitor with recommendations for defect removal. The study includes training Neural Network models on image data sets and testing them on real-world examples,

demonstrating high effectiveness in defect identification.

## 7. Concept of a System Assessing Damage in Aircraft Assembly Joints

Combining the capabilities of systems listed above with the practicality of drones and VR can significantly improve precision, efficiency and speed of inspections. The authors of this work propose a concept of a System Assessing Damage in Aircraft Assembly Joints. Schematic principle of operation of the system is presented in Fig. 1.

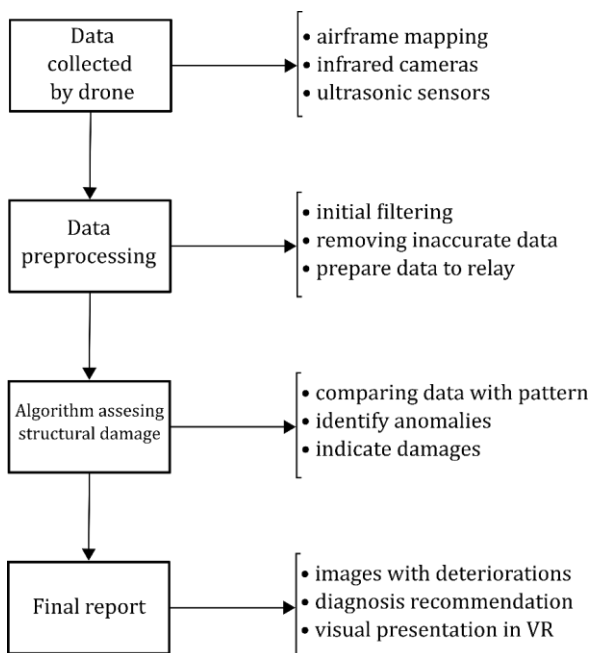


**Fig. 1.** Schematic principle of operation of the proposed System for Assessing Damage in Aircraft Assembly Joints

To proceed appropriately for this process, it is essential to accurately prepare the equipment before use by completing given checklist, e.g. checking the functionality of sensors, cameras and the drone's control surfaces. The operation should be thoroughly planned and defined in advance, establishing exact flight path covering all inspection-required areas. The paths could be predefined which may advantage in allowing the usage of multiple drones simultaneously while avoiding potential collisions.

During inspection, the drone follows the established path using sensors designed for this purpose, which ensure safe movement around the aircraft structure.

Furthermore, a certain safety margin would be set so that the appropriate distance would be maintained even in the event of measurement inaccuracies or sensor failure. The drone should collect high-resolution images and data from other sensors analysing

the structure's condition, such as infrared cameras or ultrasonic sensors. Moreover, it is crucial to ensure proper lighting of the inspected object due to the potential inaccuracies in poorly illuminated parts of the aircraft. Adequate directional lighting (e.g. LED diode) and advanced imaging technologies are essential to achieve precise and reliable detection results, minimizing the risk of overlooking critical defects. Additionally, infrared cameras and ultrasonic sensors might help eliminate some imprecise measurements caused by possible shadows. The inspection process can be significantly enhanced by employing a combination of directional lighting, infrared imaging, and ultrasonic sensing, which leads to more accurate assessments and improved time need in this process. Special attention should be given to the Light Detection and Ranging (LiDAR) system, which could be used in this case for precise mapping of the airframe (Kaartinen, Dunphy and Sadhu, 2022). LiDAR is a remote sensing technology that uses distance measurements to a target. It operates on the principle of sending out laser beams and measuring the time it takes for the light to bounce back, thus determining the distance to objects in its path. In the context of aircraft inspection and maintenance, LiDAR systems offer a non-contact method for assessing the structural integrity of aircraft components.

The data collected during the inspection undergoes preliminary analysis and filtration to remove low-quality images. The remaining data is transmitted to central data analysis systems using appropriate servers.

An example of aircraft fuselage inspection performed by drone is presented in Fig. 2.

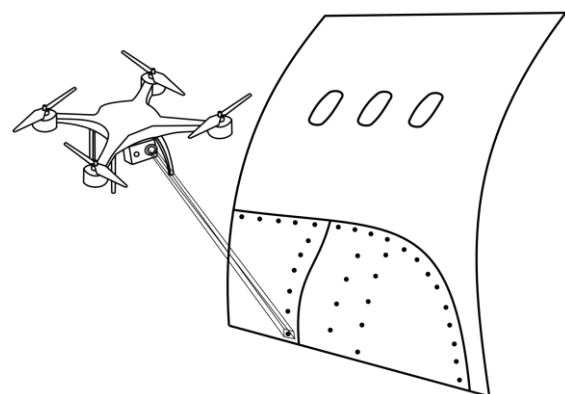


**Fig. 2.** Example of aircraft fuselage inspection performed by drone

Once the data passes the preliminary filtration, it is fed into Artificial Intelligence algorithms trained to analyse this type of information. This process begins with cleaning and preparing the data, reducing image noise and enhancing the quality of data set. After

initial analysis and sorting, CNN detect cracks, corrosion and other anomalies previously defined in the network's database. Deep Learning models classify the types of damage and assess their severity along with significance determining the potential threat to the durability of the structure.

A detailed inspection report containing images with marked damage locations, sensor data summaries, and diagnostic conclusions, is generated after the analysis. Additionally, by integrating LiDAR into aircraft inspection processes, maintenance teams can streamline their workflows, reduce inspection times and improve overall safety by identifying potential issues. Such a report can create an image of the aircraft with highlighted sensitive areas, which allows for early detection of failures or structural problems. In addition, such information may initiate optimization process of the structure in case of regularly occurring defects. It also provides a visual representation of damage locations using Augmented Reality technologies for real-time visualization of structural damage areas.

AI systems send automatic alerts to maintenance teams when critical issues are detected, allowing for the planning of maintenance tasks based on previously generated priority lists. Comparative analysis of historical data with current inspections enables the identification of trends and recurring problems.

## 8. Summary

Usage of drones and Artificial Intelligence to assess damage in aircraft assembly joints offers benefits such as increased precision, efficiency and inspection speed, which impacts on improvement of reliability and safety of aircraft. As the analysed literature shows, the proposed technologies yield satisfactory results with an adequate number of training examples. The Neural Network is capable of detecting all defects on the airframe with high probability. Additionally, continuous advancements in Machine Learning algorithms further enhance the accuracy and trustworthiness of these systems. By integrating the advanced algorithms with real-time data processing capabilities, the inspection process becomes more efficient and cost-effective, ultimately leading to increase in productivity protocols in the aviation industry.

This project involves technical challenges, such as ensuring high-quality data despite environmental conditions, continuously training and validating AI models to maintain sufficient accuracy level. The highest level of technological expertise is required to ensure adequate data. It is also crucial to comply with aviation authority regulations and guidelines con-

cerning drone operations. By extension, implementing strict safety protocols for drone operations is needed to prevent accidents. Furthermore, protection of the data and communication channels is required to prevent potential cyber threats.

Future development directions for the project point enhancing AI capabilities, such as developing self-learning systems which could continually learn from new data and improve their performance, and implementing AI systems that collaborate with inspectors in decision-making process.

Moreover, integrating advanced data analytics and machine learning techniques could further optimize inspection processes and predictive maintenance strategies, leading to greater efficiency in aircraft maintenance operations.

## References

- Amosov, O. S., Amosova, S. G., & Iochkov, I. O. (2022). Deep Neural Network Recognition of Rivet Joint Defects in Aircraft Products. *Sensors*, 22(3417). doi:<http://doi.org/10.3390/s22093417>.
- Andreopoulos, A., & Tsotsos, J. K. (2013). 50 Years of object recognition: Directions forward. *Computer Vision and Image Understanding*, 827-891. doi:<http://doi.org/10.1016/j.cviu.2013.04.005>.
- Bagheri, M., Akbarib, A., & Mirbagheri, S. A. (2019). Advanced control of membrane fouling in filtration systems using artificial intelligence and machine learning techniques: A critical review. *Process Safety and Environmental Protection*, 123, 229-252. doi:<https://doi.org/10.1016/j.psep.2019.01.01>.
- Brandoli, B., Geus, A. R., Souza, J. R., Spadon, G., Soares, A., Jose F. Rodrigues, J., . . . Matwin, S. (2021). Aircraft Fuselage Corrosion Detection Using Artificial Intelligence. *Sensors*, 21.
- Copeland, B. J., & Proudfoot, D. (2007). Artificial intelligence: History, foundations, and philosophical issues. *Philosophy of psychology and cognitive science*, 429-482. doi:<https://doi.org/10.1016/B978-044451540-7/50032-3>.
- Deng, J., Dong, W., Socher, R., Li, L.-J., Li, K., & Fei-Fei, L. (2009). ImageNet: A Large-Scale Hierarchical Image Database. *2009 IEEE Computer Society Conference on Computer Vision and Pattern Recognition*, (pp. 248-255). Miami. doi:<http://doi.org/10.1109/CVPR.2009.5206848>.
- Future of Aviation*. <https://www.icao.int/Meetings/FutureOfAviation/Pages/default.aspx> (access: 10.06.2024).
- Garbuno, D. M. *The Global Impact Of The Pratt & Whitney Engine Issues*. <https://simpleflying.com/global-impact-pratt-whitney-engine-issues/> (access: 10.06.2024).
- GROWTH AND FORECAST 2024 – 2043*. <https://www.grupooneair.com/analysis-global-growth-commercial-aviation/> (access: 10.06.2024).
- Hinton, G. E., Osindero, S., & Teh, Y.-W. (2006). A Fast Learning Algorithm for Deep Belief Nets. *Neural Computation*, 18, 1527-1554.
- Javidi, B. (2002). *Image Recognition and Classification: Algorithms, Systems, and Applications*. New York: Marcel Dekker.

- Kaartinen, E., Dunphy, K., & Sadhu, A. (2022). LiDAR-Based Structural Health Monitoring: Applications in Civil Infrastructure Systems. *Sensors* 2022, 22. doi:https://doi.org/10.3390/s22124610.
- Kaushikkumar, P. (2024). Ethical Reflections on Data-Centric AI: Balancing Benefits and Risks. *International Journal of Artificial Intelligence Research and Development*, 2(1), 1-17.
- Kuittinen, M. (2024). *Exploring the Effects of Artificial Intelligence Capabilities on Firm Performance*. Kuopio: University of Eastern Finland, Faculty of Social Sciences and Business, Department of Business.
- LeCun, Y., Bottou, L., Bengio, Y., & Haffne, P. (1998). Gradient-Based Learning Applied to Document Recognition. *Proceedings of the IEEE*, 2278-2324. doi:https://doi.org/10.1109/5.726791.
- Long, J., Shelhamer, E., & Darrell, T. (2015). Fully Convolutional Networks for Semantic Segmentation. *2015 IEEE Conference on Computer Vision and Pattern Recognition*, (pp. 3431-3440). Boston. doi:http://doi.org/10.1109/CVPR.2015.7298965.
- Milson, S., & Bruce, A. (2024). The Intelligent Data Era: How AI is Shaping the Future of Big Data. *EasyChair Preprint no. 11896*.
- National Transport Safety Board. (2024). *Aviation Investigation Preliminary Report – Accident Number: DCA24MA063*.
- Nex, F., & Remondino, F. (2014). UAV for 3D mapping applications: A review. *Applied Geomatics*, 6. doi:http://doi.org/10.1007/s12518-013-0120-x.
- Pargieła, K. (2023). Optimising UAV Data Acquisition and Processing for Photogrammetry: A Review. *GEOMATICS AND ENVIRONMENTAL ENGINEERING*, 17(3), pp. 29-59. doi:https://doi.org/10.7494/geom.2023.17.3.29.
- Sun, H., Yan, H., Hassanalian, M., Zhang, J., & Abdelkef, A. (2023). UAV Platforms for Data Acquisition and Intervention Practices in Forestry: Towards More Intelligent Applications. *Aerospace*. doi:https://doi.org/10.3390/aerospace10030317.
- Yao, H., Qin, R., & Chen, X. (2019). Unmanned Aerial Vehicle for Remote Sensing Applications – A Review. *Remote Sens*, 11. doi:https://doi.org/10.3390/rs11121443.
- Zachariah, R. A., Sharma, S., & Kumar, V. (2023). Systematic review of passenger demand forecasting in aviation industry. *Multimedia Tools and Applications*, 1-37. doi:https://doi.org/10.1007/s11042-023-15552-1.
- Zhao, H., Xi, J., Zheng, K., Shi, Z., Lin, J., Nikbin, K., . . . Wang, B. (2020). A review on solid riveting techniques in aircraft assembling. *Manufacturing Review*, 7(40).
- Zuchniak, K., Dzwiniel, W., Majerz, E., Pasternak, A., & Dragan, K. (2021). Corrosion detection on aircraft fuselage with multi-teacher knowledge distillation. *Computational Science – ICCS 2021*.
- Zwęgliński, T. (2020). The Use of Drones in Disaster Aerial Needs Reconnaissance and Damage Assessment – Three-Dimensional Modeling and Orthophoto Map Study. *Sustainability*, 12. doi:http://doi.org/10.3390/su12156080.

DOCUMENT  
CREATED  
WITH



PDF  
COMBINER

PDF Combiner is a free application that you can use to combine multiple PDF documents into one.

Three simple steps are needed to merge several PDF documents. First, we must add files to the program. This can be done using the Add files button or by dragging files to the list via the Drag and Drop mechanism. Then you need to adjust the order of files if list order is not suitable. The last step is joining files. To do this, click button Combine PDFs.

Main features:

**secure PDF merging** - everything is done on your computer and documents are not sent anywhere

**simplicity** - you need to follow three steps to merge documents

**possibility to rearrange document** - change the order of merged documents and page selection

**reliability** - application is not modifying a content of merged documents.

Visit the homepage to download the application:

[www.jankowskimichal.pl/pdf-combiner](http://www.jankowskimichal.pl/pdf-combiner)

To remove this page from your document, please donate a project.